ATLAS diboson results

Eleni Mountricha
[Brookhaven National Laboratory]

on behalf of the
ATLAS collaboration

Higgs Hunting 2015
30 July - 1 August, 2015

Higgs to dibosons @ LHC

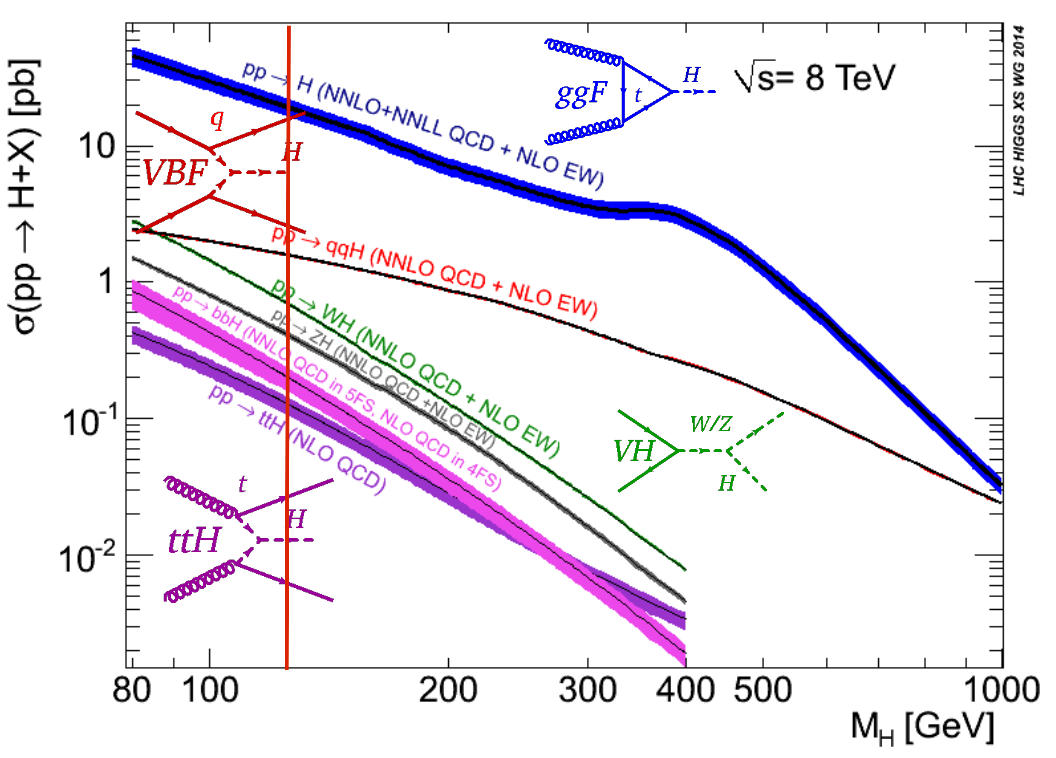

- Cross sections calculated @NNLO with NNLL QCD & NLO EW for main production mode [gluon fusion]

high rate with lepton final states but not fully reconstructed

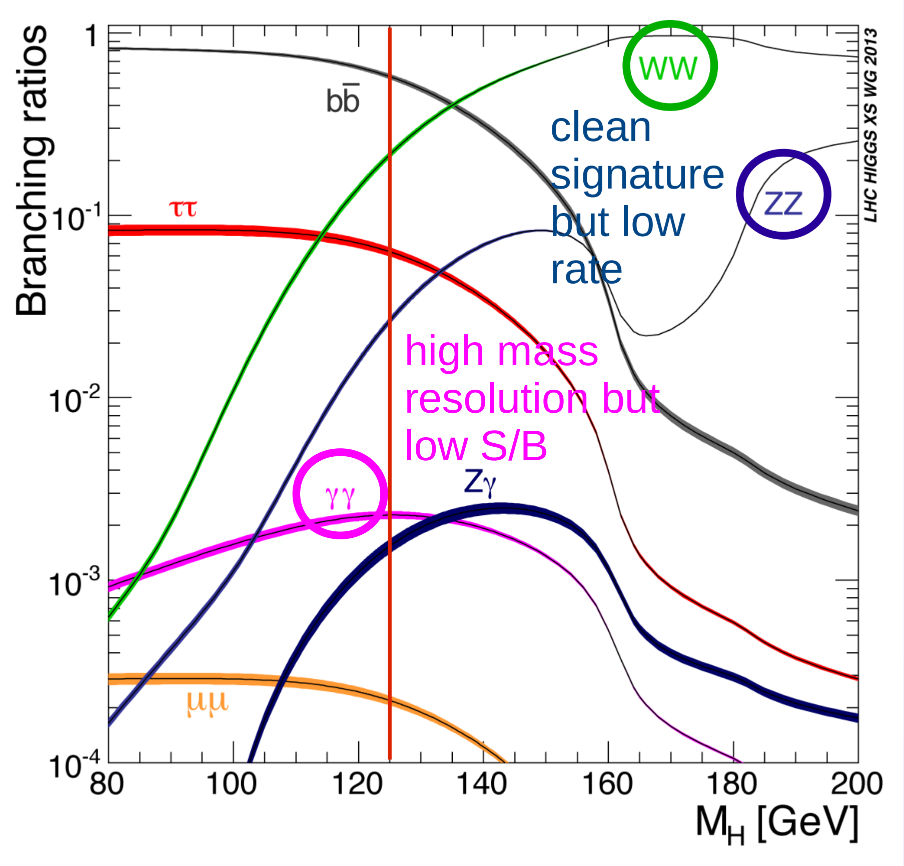

- Higgs di-boson decays dominated by WW [BR (H -> WW) ~ 22%]
- Higgs width far smaller [~4 MeV] than experimental resolution

Phys. Rev. D90, 112015 (2014)

H→γγ selection

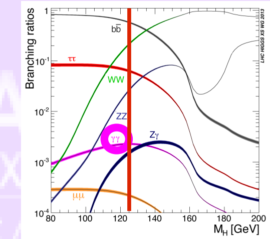

2 isolated photons
$p_T / m_{\gamma\gamma} > 0.35, 0.25$

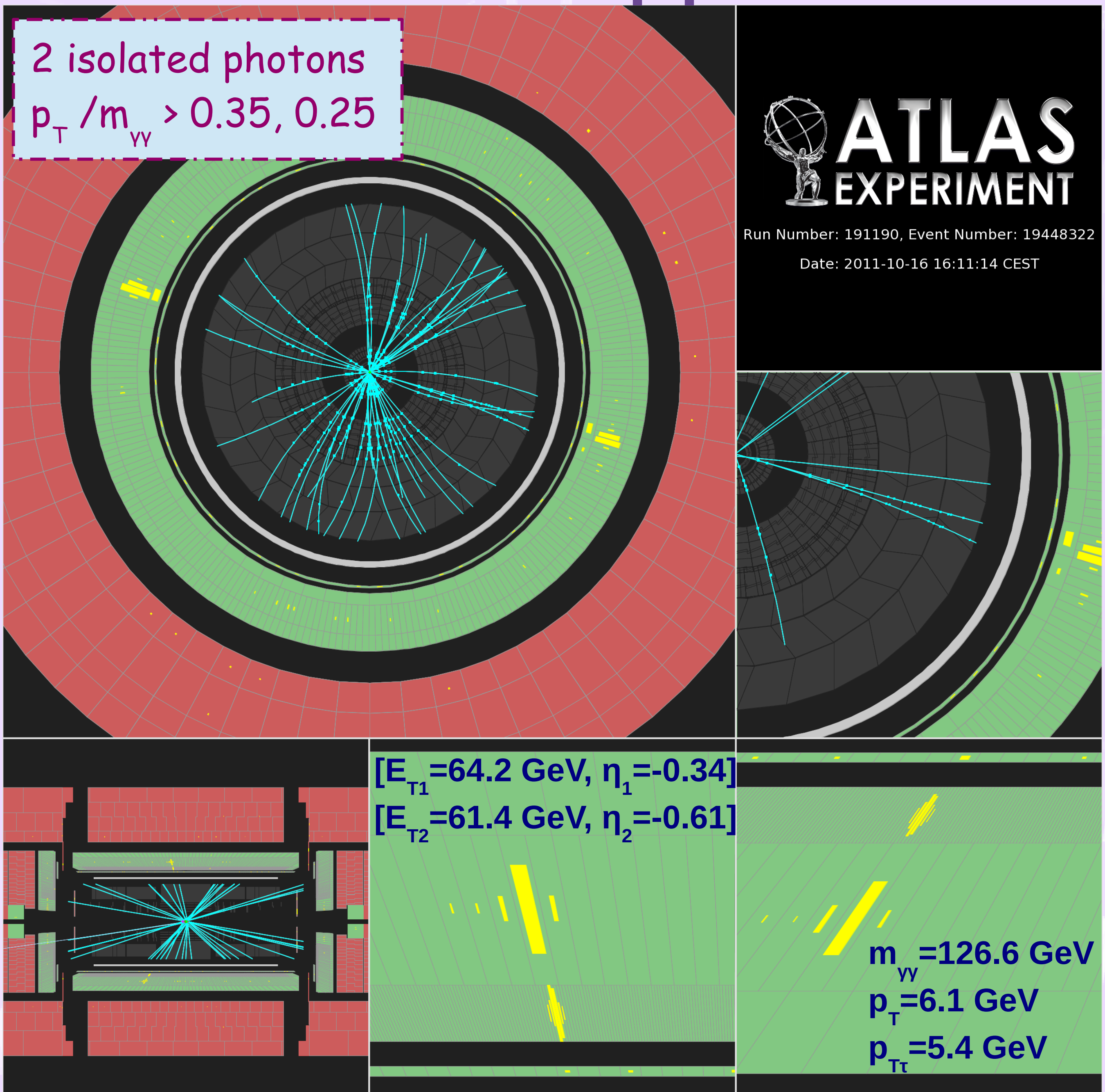

- Calorimeter pointing information

$$m_{\gamma\gamma} = \sqrt{2E_1E_2(1-\cos\alpha)}$$

- Categories according: mass resolution, S/B and production modes sensitivity

Improvements in: event selection, event categorization but also in energy calibration brought 10% improvement in the expected signal strength uncertainty

Phys. Rev. D90, 112015 (2014)

H→γγ signal

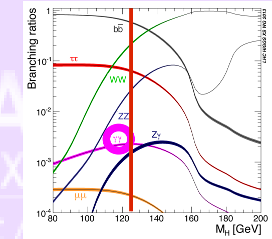

5.2σ significance
(4.6σ expected)

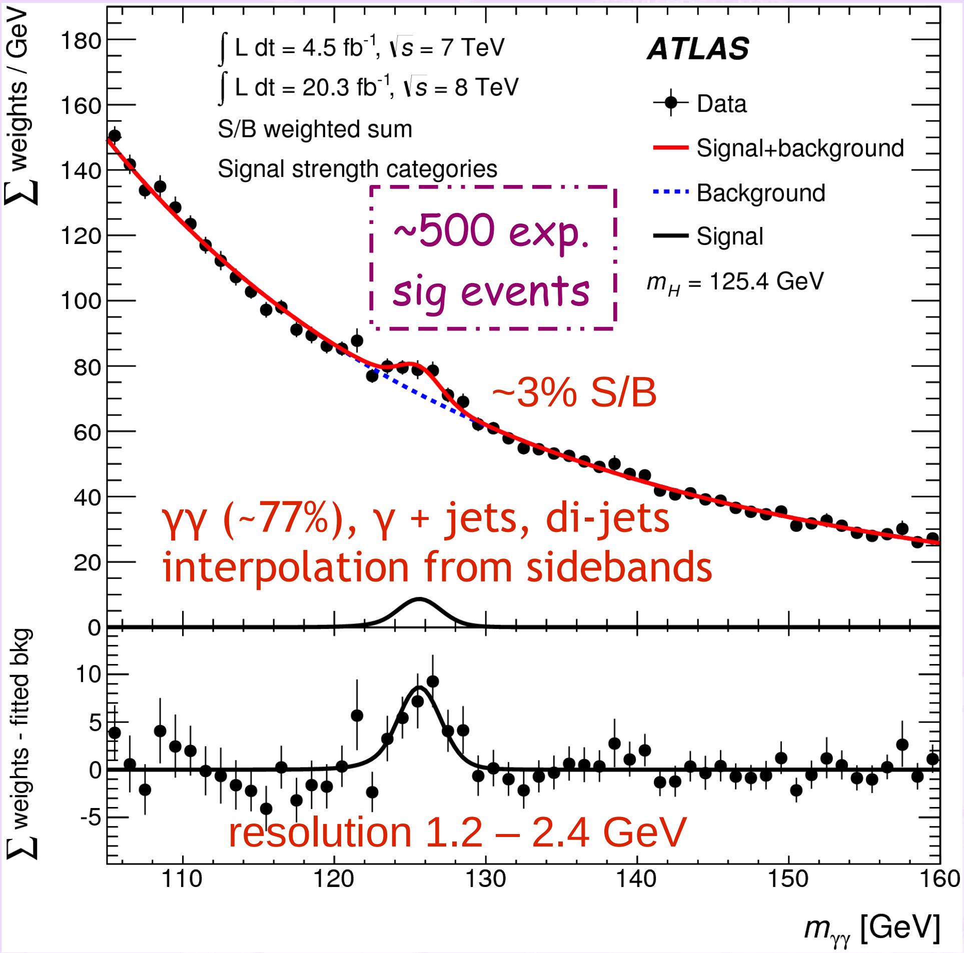

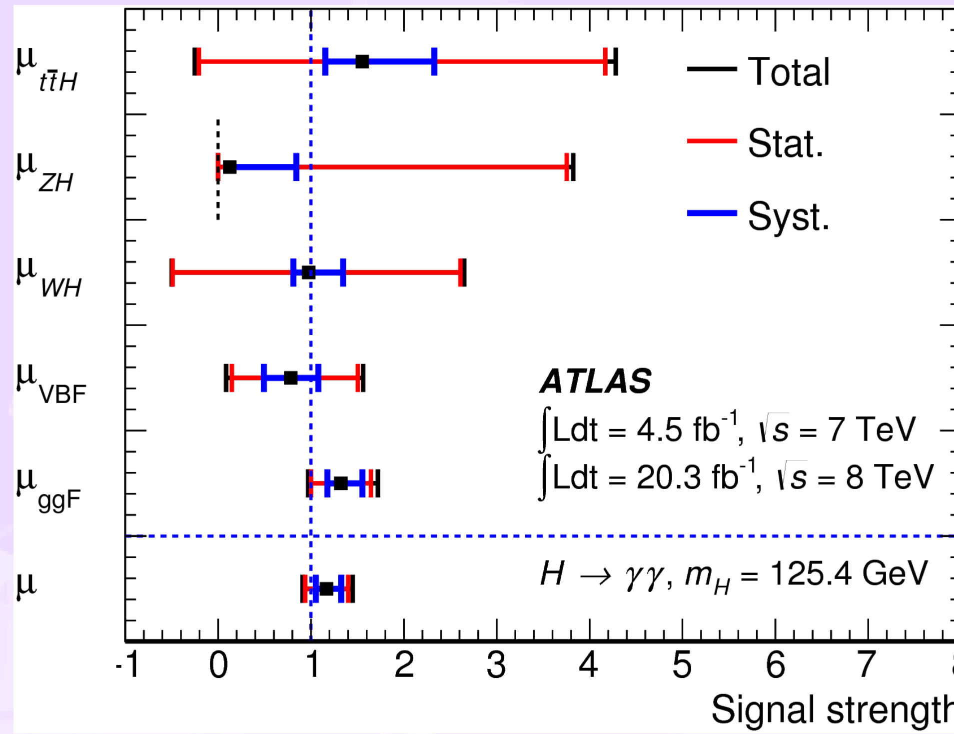

$\mu = 1.17 \pm 0.27$

$m_H = 125.98 \pm 0.42\ (\text{stat}) \pm 0.28\ (\text{syst})$ GeV

- Dominant systematic uncertainties: photon energy scale

- Dominant systematic uncertainties: theoretical [categories migration, QCD scale, PDF and BR] and photon energy resolution

Phys. Rev. D 91, 012006 (2015)

H→ZZ*→4l selection

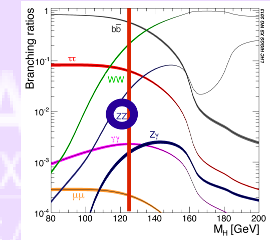

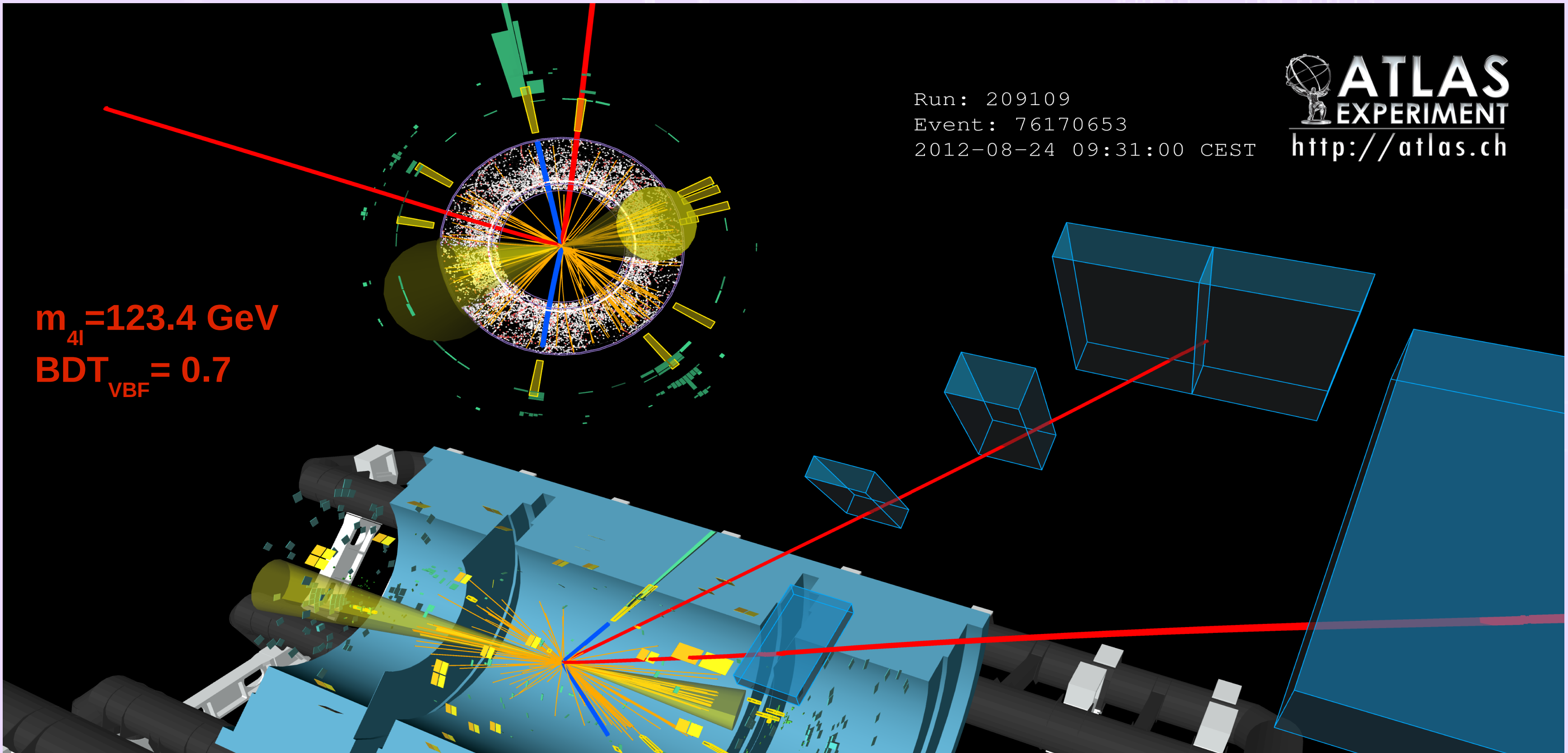

2 isolated lepton pairs

p_T > 6(7)/10/15/20 GeV, for μ(e), m_{12} > 50 GeV, m_{34} > 12 GeV

- Categories according: lepton flavor and to production modes sensitivity

Improvements in event selection and categorization [use of multivariate discriminants and 2-dimensional fit] and in the electron ID and energy resolution brought a 15% improvement on the expected signal strength uncertainty and 8% on the expected statistical uncertainty of the mass

Phys. Rev. D 91, 012006 (2015)

H→ZZ*→4l signal

8.1σ significance
(6.2σ expected)

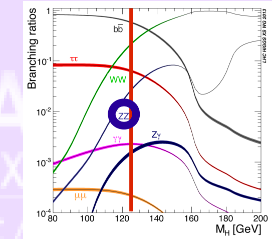

$\mu = 1.44\,^{+0.40}_{-0.33}$

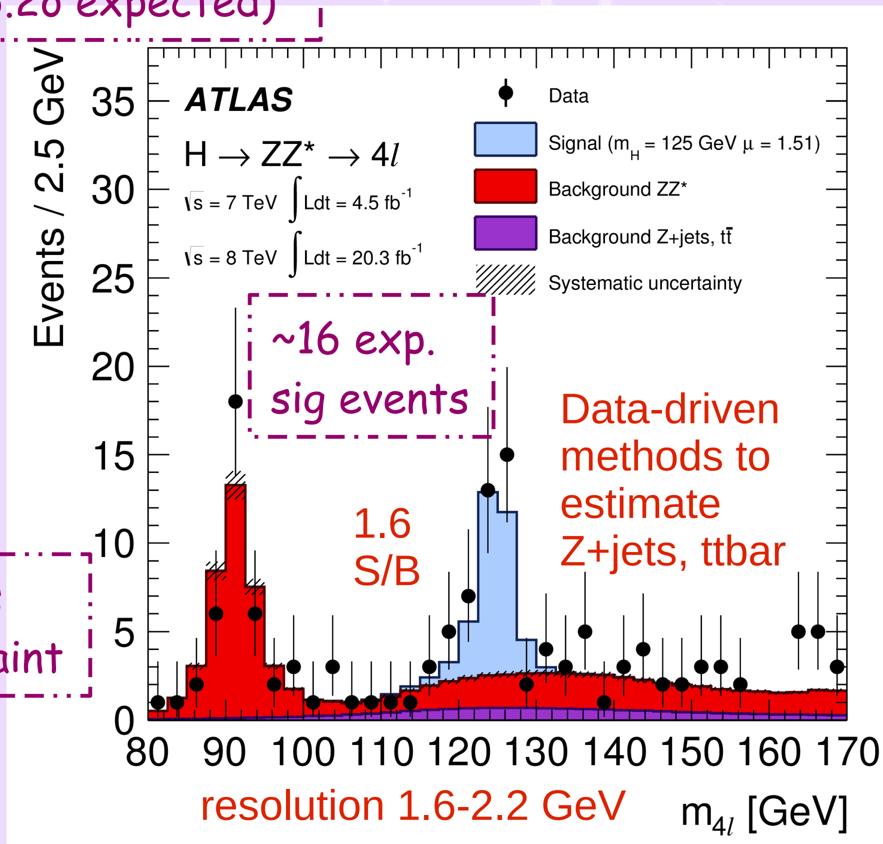

Z-mass constraint

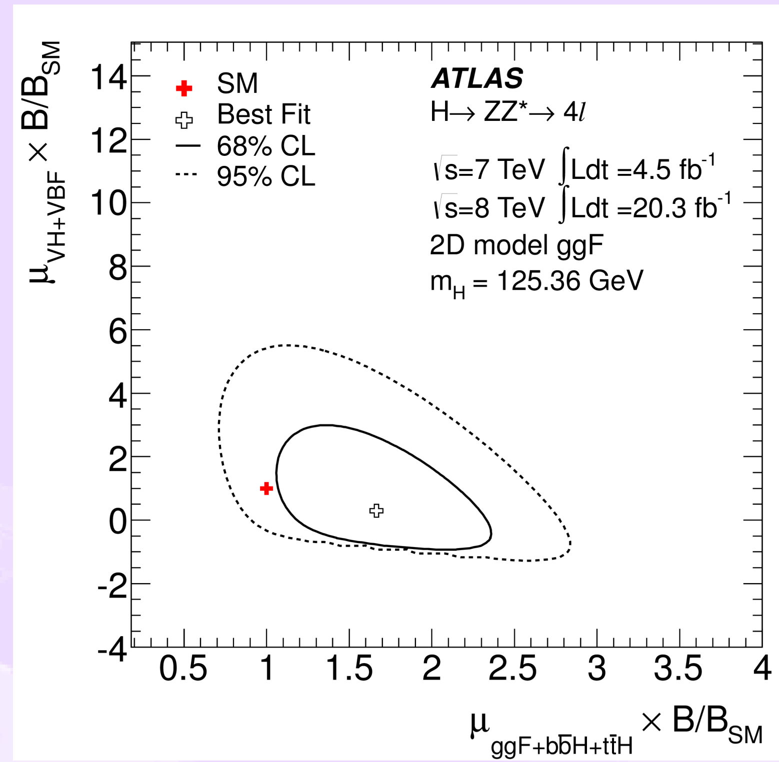

BDT discriminant against ZZ* background

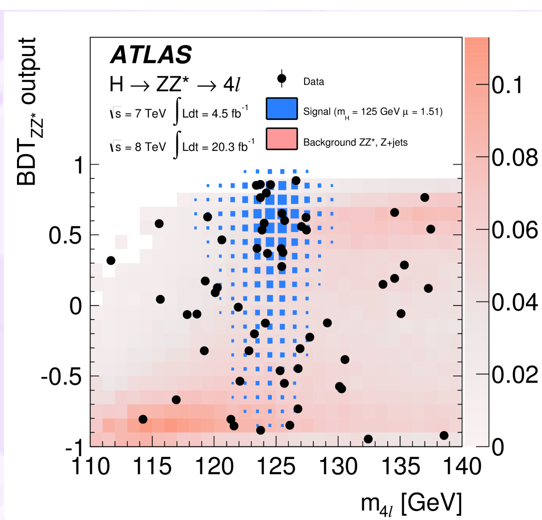

- Dominant systematic uncertainties: theoretical [jet multiplicity, QCD scale, PDF, BR] and jet energy scale

m_H = 124.51 ± 0.52 (stat) ± 0.06 (syst) GeV

- Dominant systematic uncertainties: electron/muon energy/momentum scale

Phys. Rev. D 92, 012006 (2015)

$H \rightarrow WW^* \rightarrow l\nu l\nu$ selection

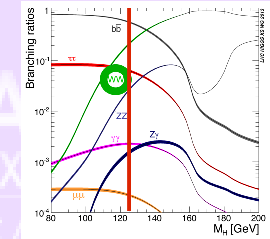

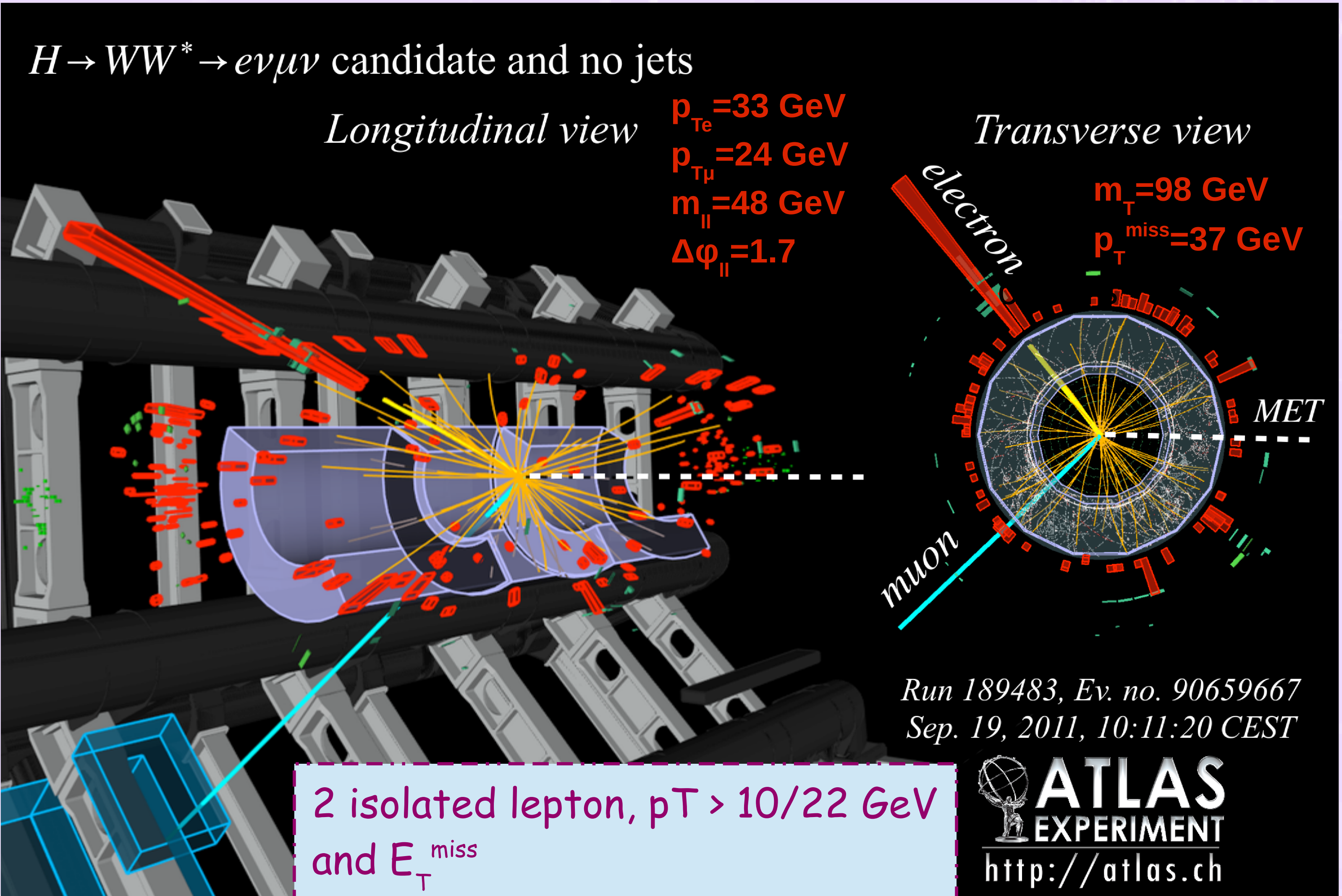

2 isolated lepton, pT > 10/22 GeV and E_T^{miss}

- Categories according: background composition [Njets (0, 1, ≥2), lepton flavor, m_{ll} and $p_{T,l2}$], production mode sensitivity

Improvements in event selection and categorization [signal acceptance, background estimation/modeling] brought a 50% gain on the expected significance and 30% improvement in the expected signal strength uncertainty

Phys. Rev. D 92, 012006 (2015)

H→WW* signal

6.5σ significance
(5.9σ expected)

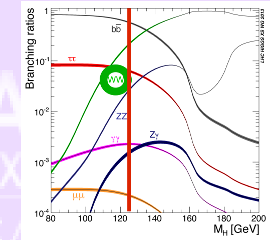

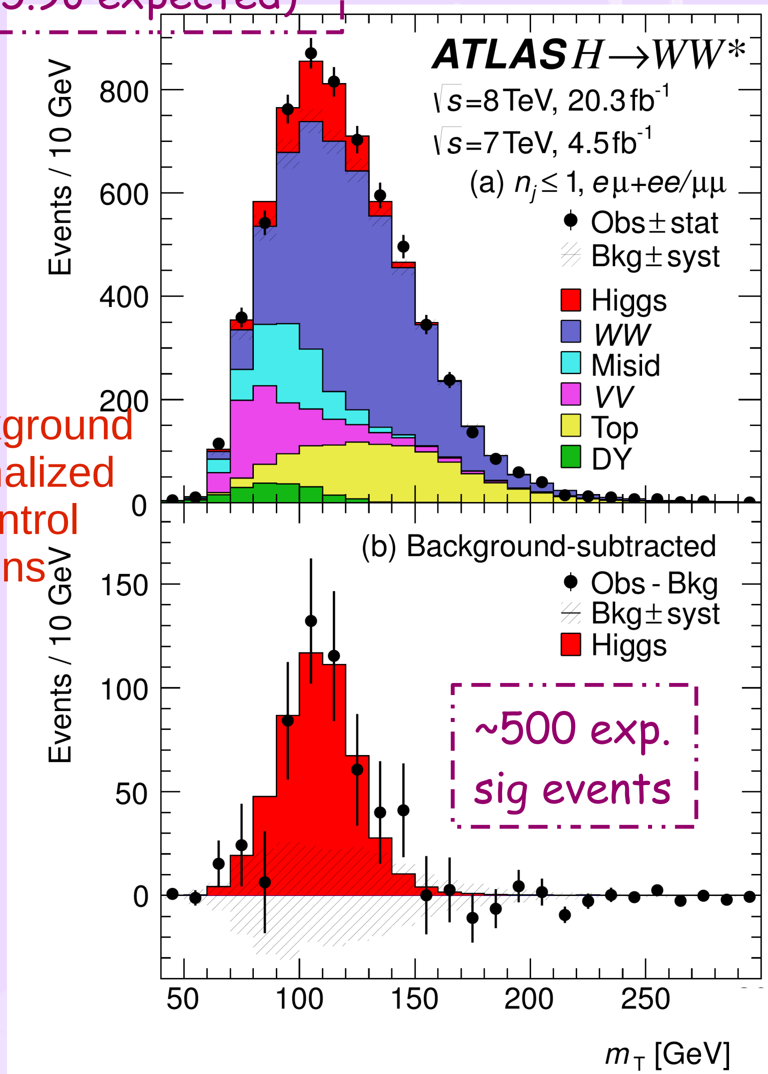

Background normalized in control regions

~500 exp. sig events

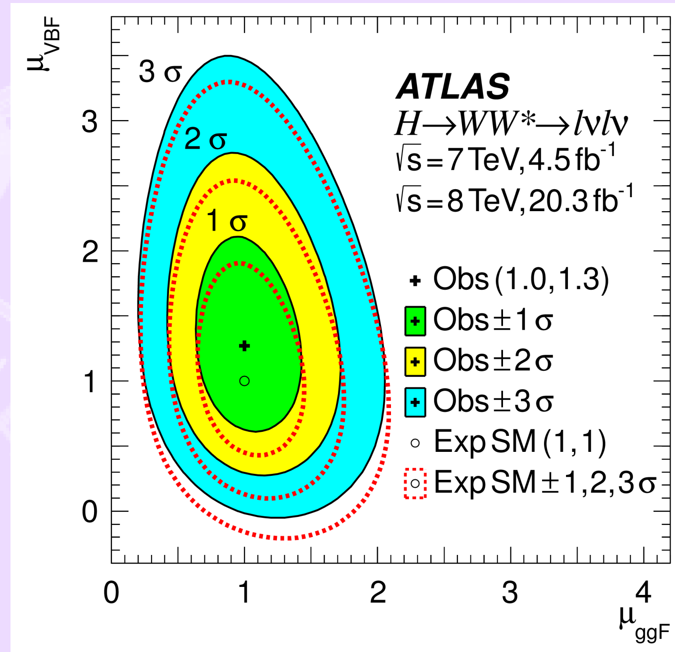

VBF production
3.2σ significance
(2.7σ expected)

$\mu = 1.16^{+0.24}_{-0.21}$

VH analysis sensitive to κ_F/κ_V relative sign

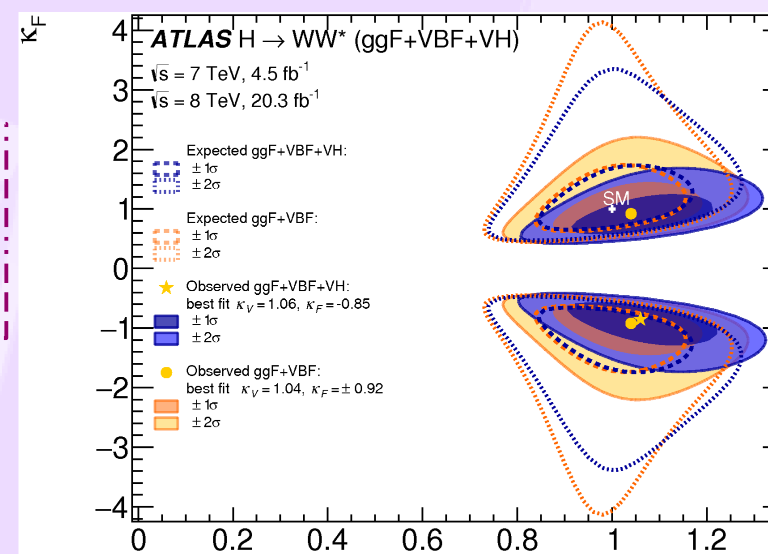

arXiv:1506.06641

- Dominant systematic uncertainties: theoretical [QCD scale, PDF, UE/PS, jet binning/veto], including theory ones on background extrapolation factors and normalization

Phys. Rev. D90, 052004 (2014)

Higgs mass measurement

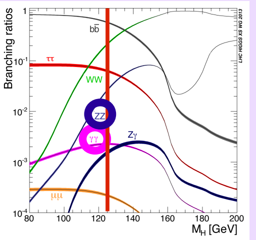

- Fully reconstructed and high resolution: $H \rightarrow \gamma\gamma$ and $H \rightarrow ZZ^* \rightarrow 4l$

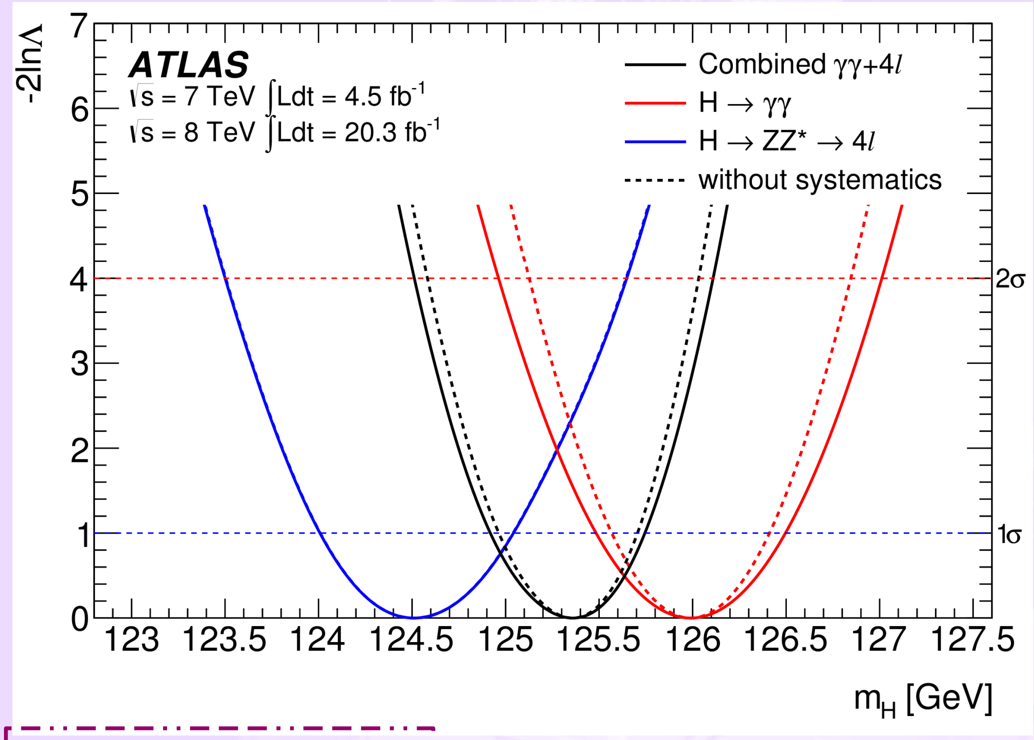

compatibility @~2σ

m_H = 125.36 ± 0.37 (stat) ± 0.18 (syst) GeV

- Dominant systematic uncertainties: photon energy scale [material, calibration, non-linearity and shower shapes]

syst uncertainties @ 1‰

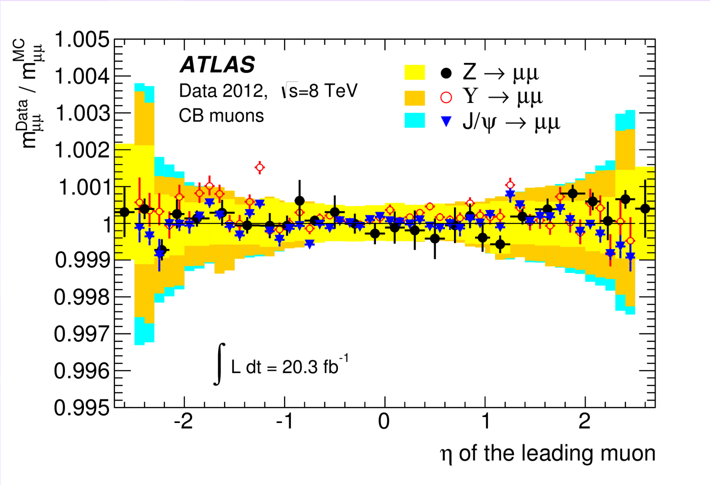

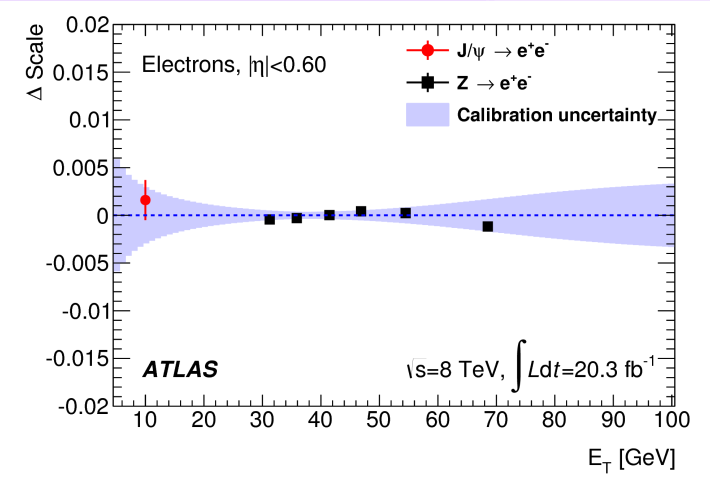

- Lepton and photon energy scales under control

Fiducial differential production

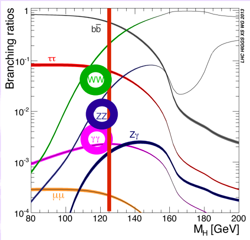

- Differential cross sections probe theoretical modeling [pQCD, PDFs], relative contribution of production modes and non-SM interactions

$$\frac{d\sigma_{\mathrm{fid},i}}{dx_i} = \frac{n_i^{\mathrm{sig}}}{c_i \cdot \mathcal{L}_{\mathrm{int}} \cdot \Delta x_i}$$

PLB 738 234-253 (2014)

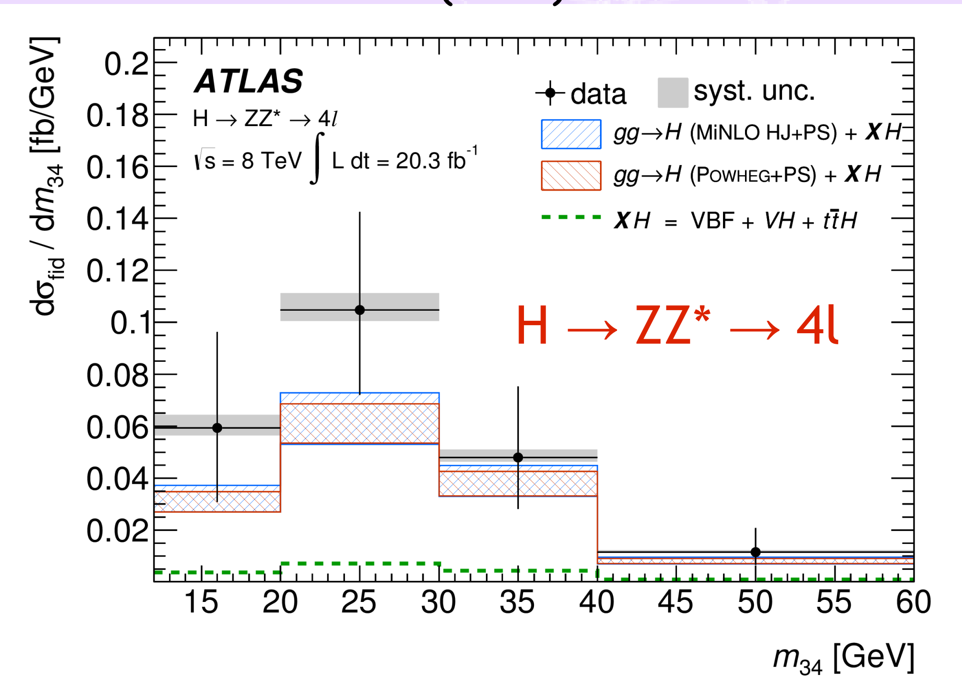

JHEP 09, 112 (2014)

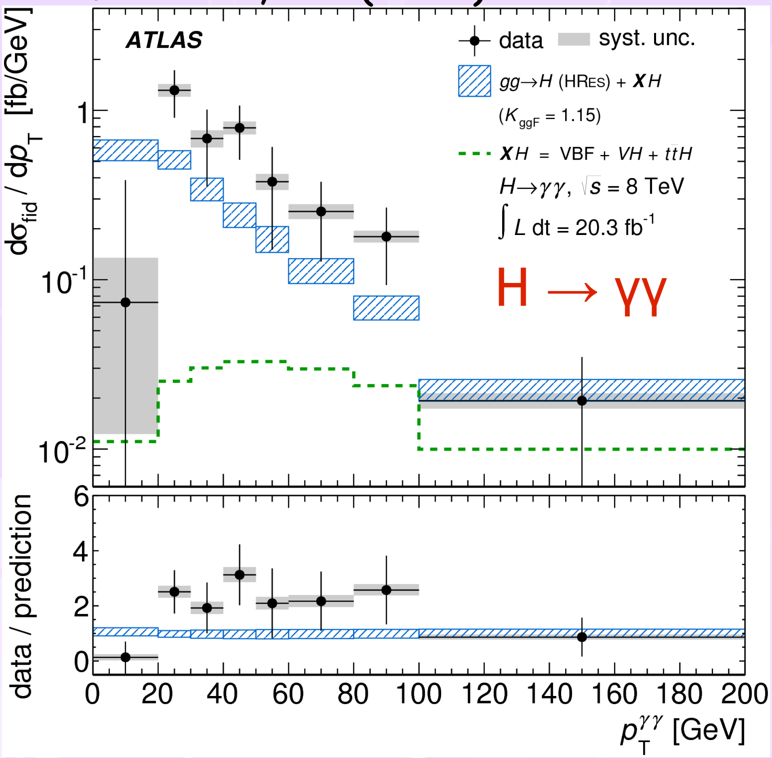

- H→WW*: $\sigma^{ggf}_{fid,0j} = 27.6\ ^{+5.4}_{-5.3}(\mathrm{stat.})\ ^{+4.1}_{-3.9}(\mathrm{syst.})$ fb, 19.9 ± 3.3 fb expected

  $\sigma^{ggf}_{fid,1j} = 8.3\ ^{+3.1}_{-3.0}(\mathrm{stat.})\ ^{+3.1}_{-3.0}(\mathrm{syst.})$ fb, 7.3 ± 1.8 fb expected

Phys. Rev. D 92, 012006 (2015)

arXiv:1504.05833 - PRL

Higgs total production

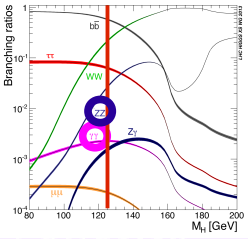

- Total production cross sections measured in ATLAS:

$$\sigma_{pp\to H} = 33.0 \pm 5.3\ (\text{stat}) \pm 1.6\ (\text{sys})\ \text{pb}$$

$H \to \gamma\gamma$
$H \to ZZ \to 4l$

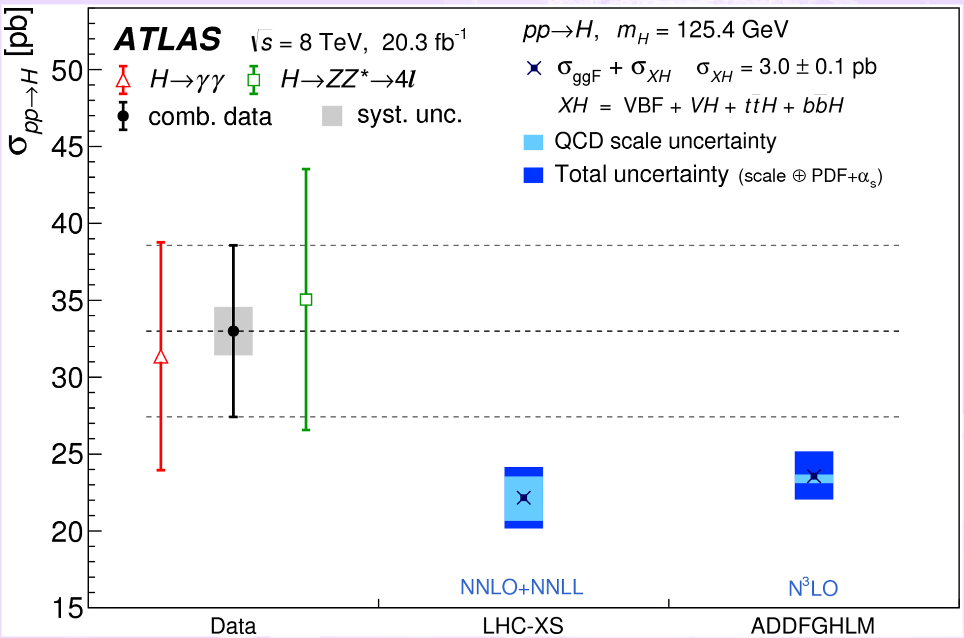

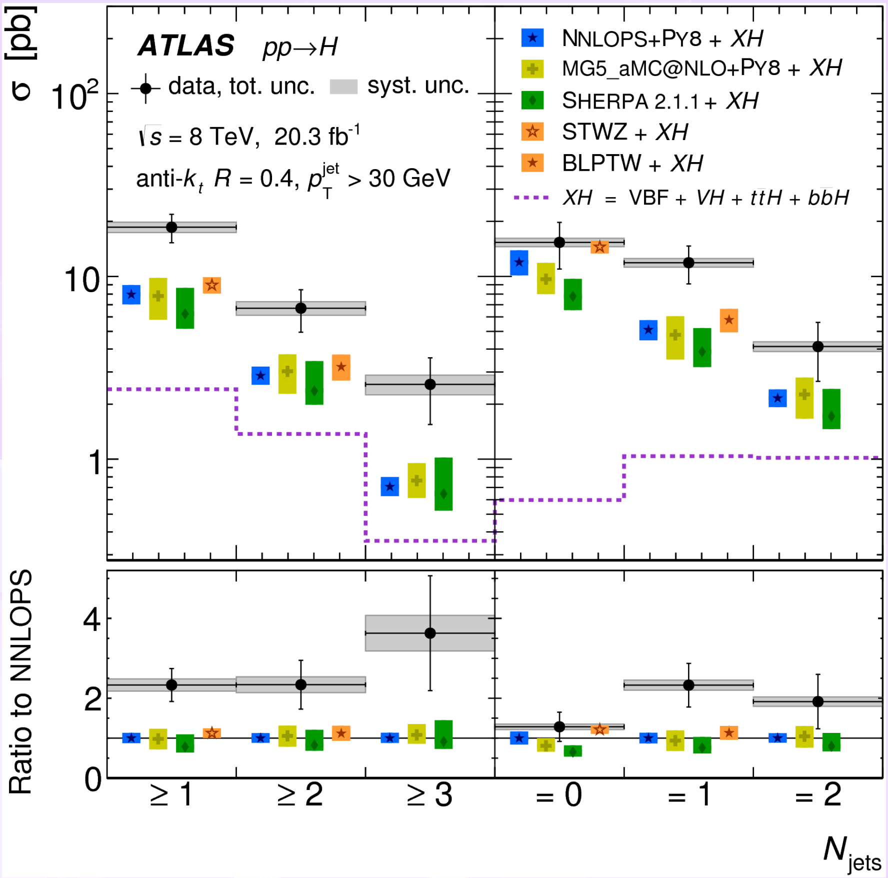

- Measured production in data is larger than state-of-the-art predictions; p-values for the agreement are 5.5% (9.0%) for LHC-XS (ADDFGHLM)

- Very good agreement in the shapes

Effective Field Theory

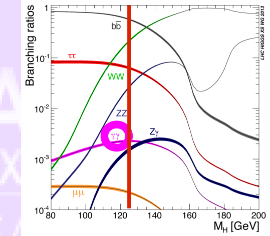

H → γγ

- Probe BSM CP-even and CP-odd interactions using five differential cross sections in the context of the Effective Field Theory framework and the Strongly Interacting Light Higgs (SILH) formulation:

$$\mathcal{L} = \bar{c}_\gamma O_\gamma + \bar{c}_g O_g + \bar{c}_{HW} O_{HW} + \bar{c}_{HB} O_{HB} + \tilde{c}_\gamma \tilde{O}_\gamma + \tilde{c}_g \tilde{O}_g + \tilde{c}_{HW} \tilde{O}_{HW} + \tilde{c}_{HB} \tilde{O}_{HB}$$

Wilson coefficients specifying the strength of the new interactions

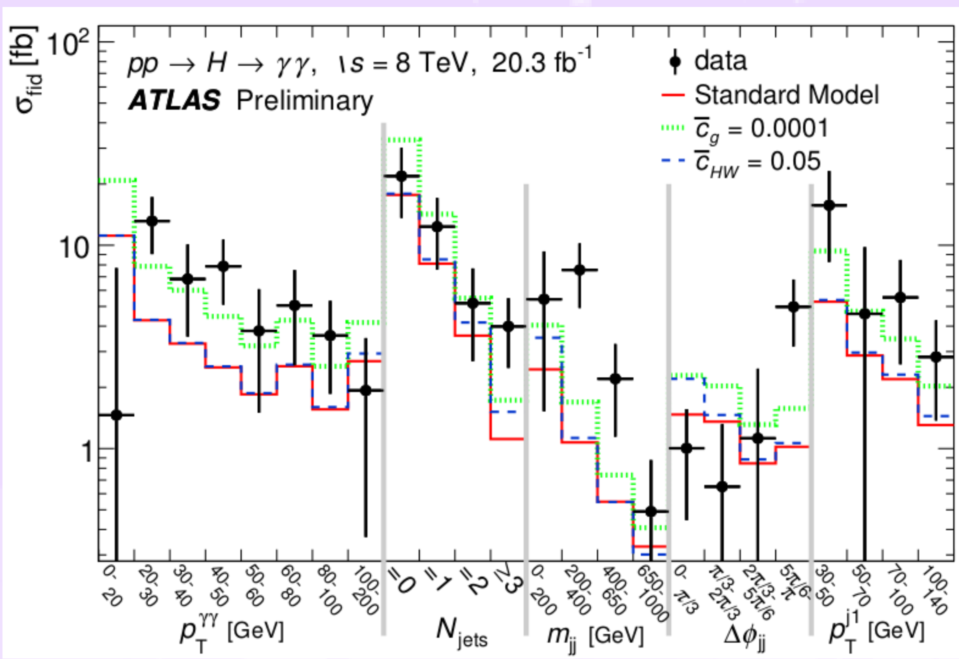

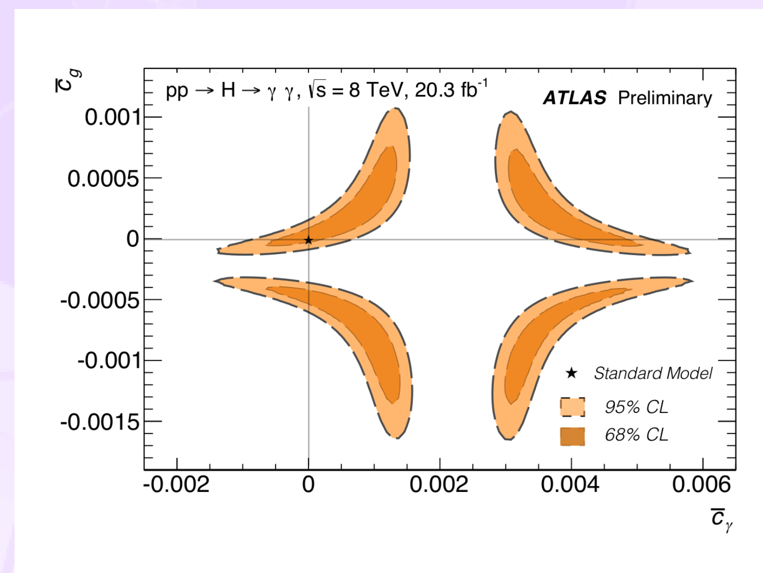

- Strong limits arising from the inclusion of rate and jet kinematic information wrt limits set from the spin/CP analysis – talk by R.Polifka/L.Pedersen

Eur. Phys. J. C (2015) 75:335

Higgs width measurements

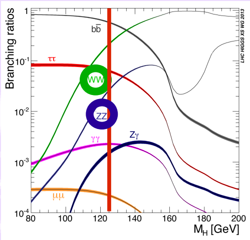

- Direct measurement limited by experimental resolution [1-2 GeV]
  Γ_H ($H\to\gamma\gamma$) < 5.0 GeV @ 95% CL, 4.2 GeV expected
  Γ_H ($H\to ZZ^*\to 4l$) < 2.6 GeV @ 95% CL, 3.5 GeV expected

- Indirect measurement from the off-shell production

$$\boxed{\mu_{\text{off-shell}}(\hat{s})} \equiv \frac{\sigma^{gg\to H^*\to VV}_{\text{off-shell}}(\hat{s})}{\sigma^{gg\to H^*\to VV}_{\text{off-shell, SM}}(\hat{s})} = \kappa^2_{g,\text{off-shell}}(\hat{s})\cdot\kappa^2_{V,\text{off-shell}}(\hat{s})$$

$$\boxed{\mu_{\text{on-shell}}} \equiv \frac{\sigma^{gg\to H\to VV}_{\text{on-shell}}}{\sigma^{gg\to H\to VV}_{\text{on-shell, SM}}} = \frac{\kappa^2_{g,\text{on-shell}}\cdot\kappa^2_{V,\text{on-shell}}}{\boxed{\Gamma_H/\Gamma_H^{\text{SM}}}}$$

- Assumption: off-shell couplings at least as large as on-shell [sensitive to contributions from new physics]
  → limit on Higgs width

- Interference of off-shell signal with gluon-initiated ZZ background

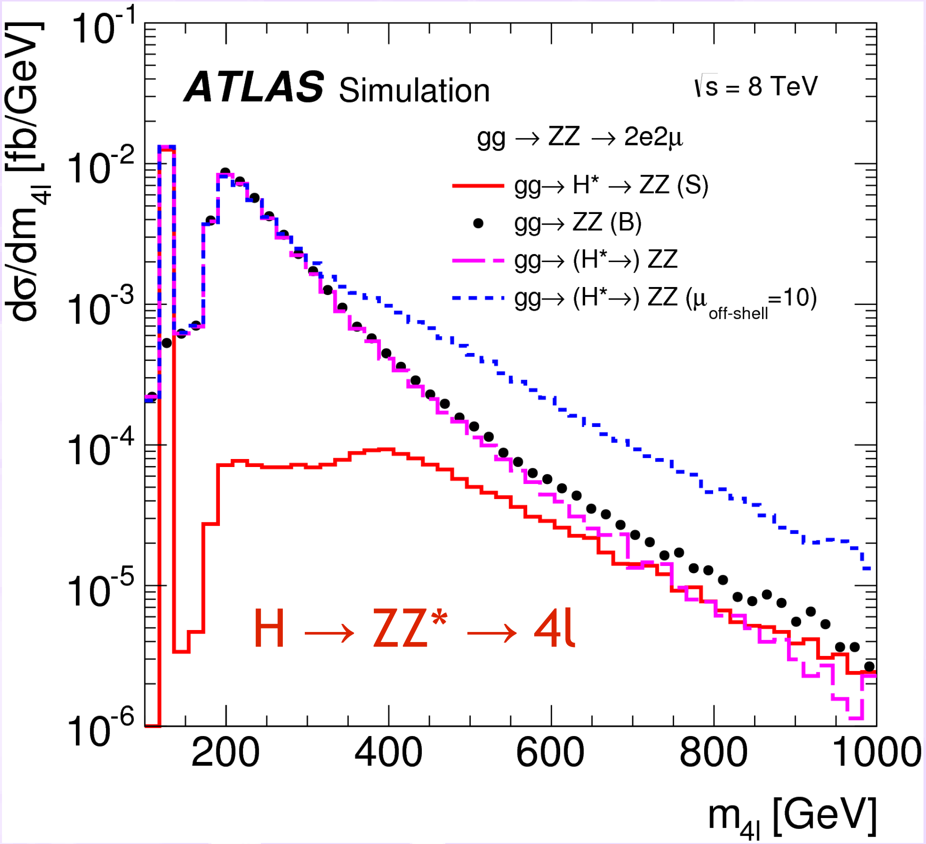

Eur. Phys. J. C (2015) 75:335

Width indirect measurement

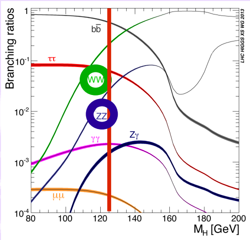

H → ZZ* → 4l

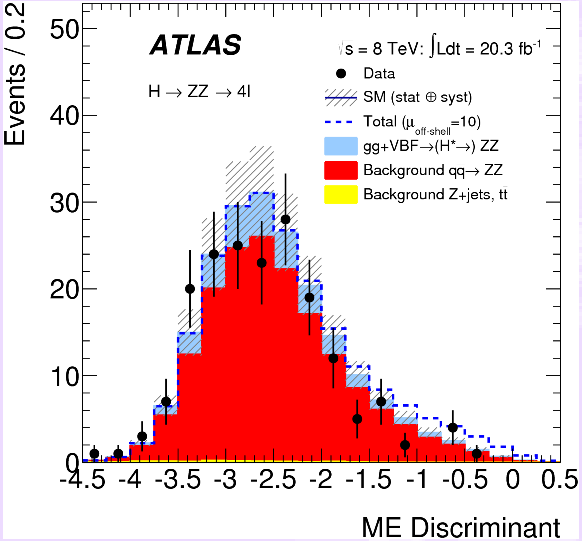

H → ZZ* → llνν

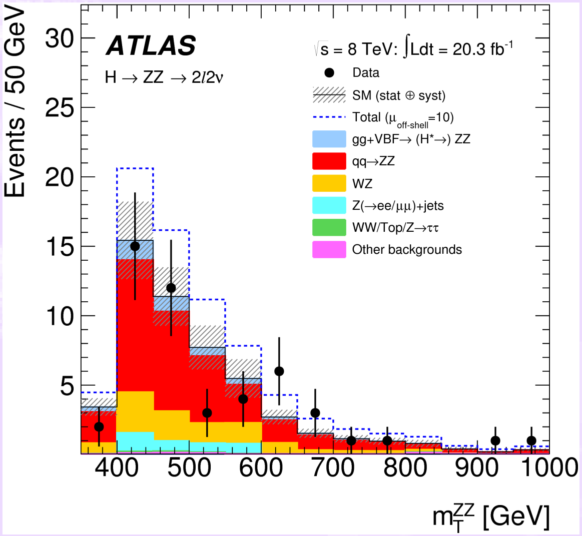

H → WW* → eνμν

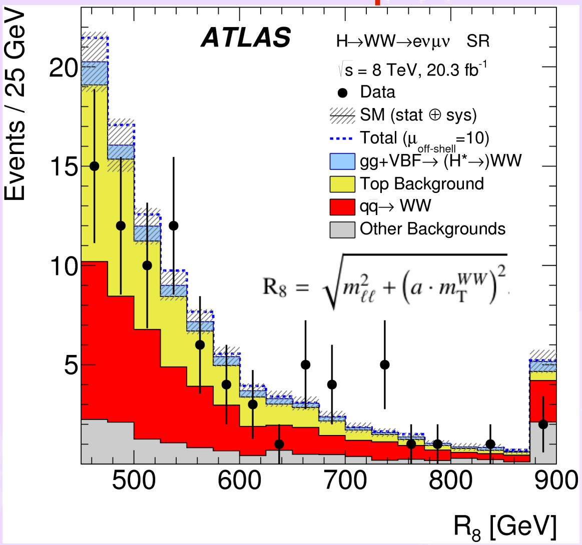

- Sensitive to higher order QCD corrections for gg→VV [unknown $\kappa_{gg\to VV}$ factor]
- Dominant systematic uncertainties: theoretical uncertainties on gg→H→VV, gg/qq→VV and their interference

$\mu_{offshell}$ < 6.2 (8.2) @ 95% CL obs (exp)

Γ_H < 22.7 (33.0) MeV @ 95% CL obs (exp)

R^B_H=1

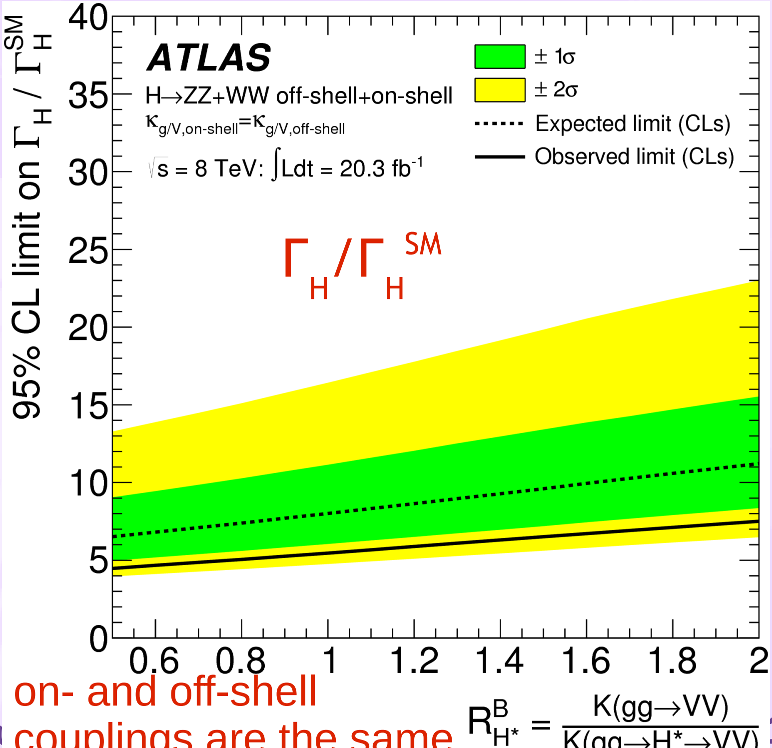

on- and off-shell couplings are the same

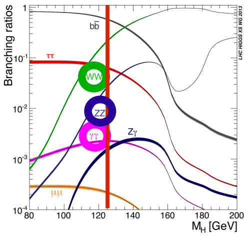

Higgs spin/parity

- SM $J^P = 0^+$ tested against alternative models [non-SM spin-0 and spin-2 with different choices of QCD couplings]

Angular distribution variables sensitive to spin/CP determination

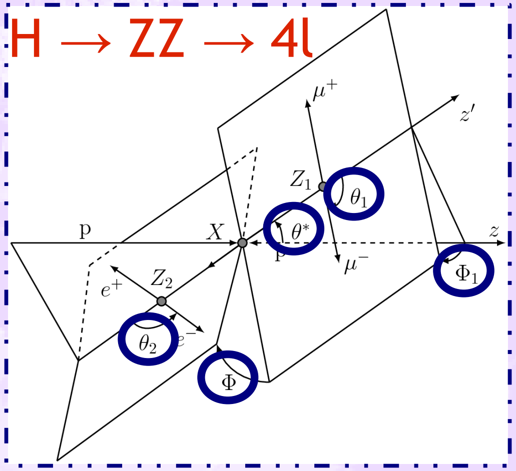

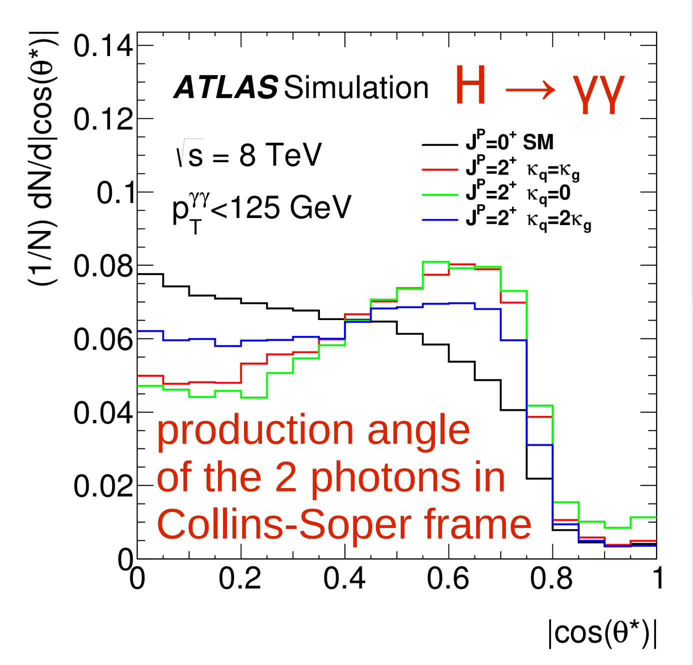

- Probe possible presence of BSM terms in the HVV tensor structure of the spin-0 resonance

$$\mathcal{L}_0^V = \{c_\alpha \kappa_{SM}[\frac{1}{2}g_{HZZ}Z_\mu Z^\mu + g_{HWW}W_\mu^+ W^-\mu] - \frac{1}{4}\frac{1}{\Lambda}[c_\alpha \kappa_{HZZ}Z_{\mu\nu}Z^{\mu\nu} + s_\alpha \kappa_{AZZ}Z_{\mu\nu}\tilde{Z}^{\mu\nu}] - \frac{1}{2}\frac{1}{\Lambda}[c_\alpha \kappa_{HWW}W_{\mu\nu}^+ W^{-\mu\nu} + s_\alpha \kappa_{AWW}W_{\mu\nu}^+ \tilde{Z}^{-\mu\nu}]\}$$

SM coupling

BSM CP-odd coupling

BSM CP-even coupling

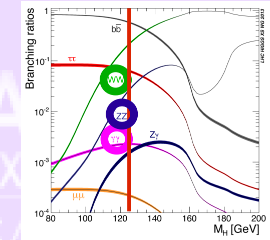

Higgs spin/parity

- SM $J^P = 0^+$ tested against alternative models [non-SM spin-0 and spin-2 with different choices of QCD couplings]

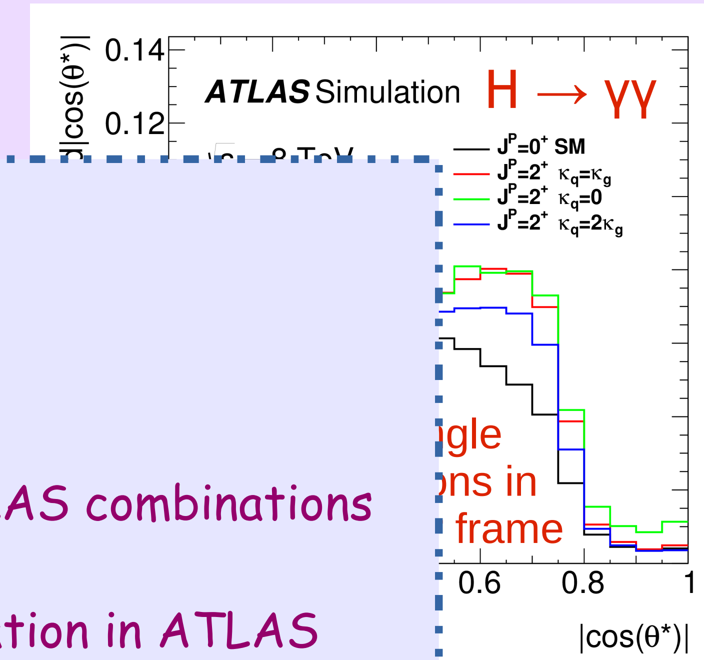

Angular dis
variables s
spin/CP de

gle
ons in
frame

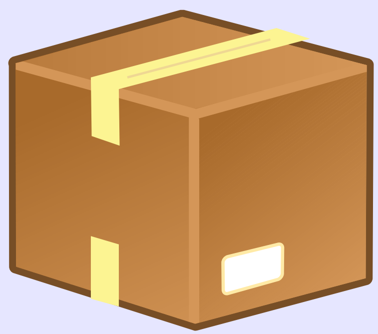

R. Polifka – ATLAS combinations

L. Egholm Pedersen – Spin/CP Combination in ATLAS

- Probe possible presence of BSM terms in the HVV tensor structure of the spin-0 resonance

$$\mathcal{L}_0^V = \{c_\alpha \kappa_{SM}[\frac{1}{2}g_{HZZ}Z_\mu Z^\mu + g_{HWW}W^+_\mu W^-\mu] - \frac{1}{4}\frac{1}{\Lambda}[c_\alpha\kappa_{HZZ}Z_{\mu\nu}Z^{\mu\nu} + s_\alpha\kappa_{AZZ}Z_{\mu\nu}\tilde{Z}^{\mu\nu}] - \frac{1}{2}\frac{1}{\Lambda}[c_\alpha\kappa_{HWW}W^+_{\mu\nu}W^{-\mu\nu} + s_\alpha\kappa_{AWW}W^+_{\mu\nu}\tilde{Z}^{-\mu\nu}]\}$$

SM coupling

BSM CP-odd coupling

BSM CP-even coupling

Conclusions

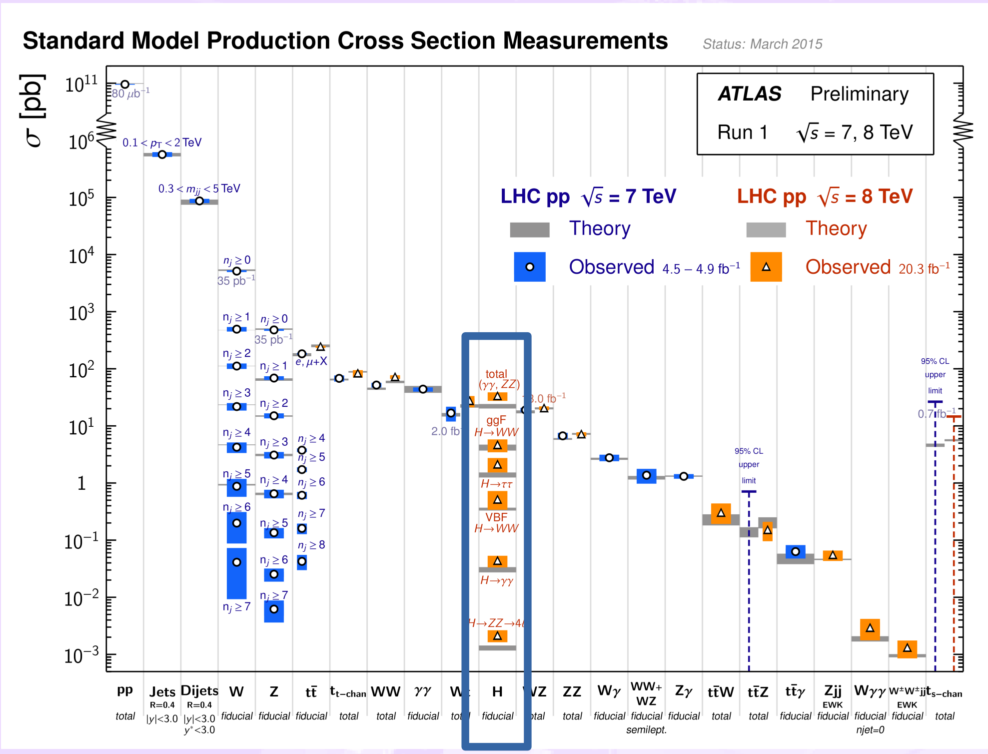

- Higgs boson properties precision measurements era! [m_H, $\sigma_{pp\to H}$, J^P, couplings]
- Di-boson channels leading the precision!
- More to come: Run II has just started!!

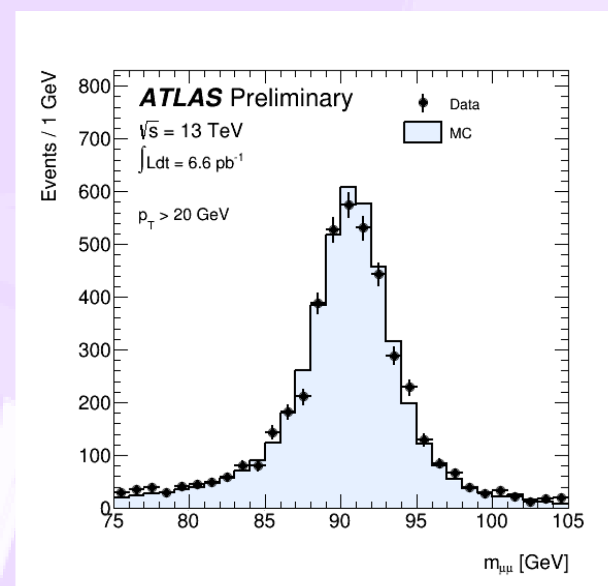

ATLAS results to follow:

- K. Nakamura - di-fermions
- M. Beckingham - BSM
- R. Polifka – combinations
- J. Leveque – RunII prospect
- D. Di Valentino – HL-LHC
- L.E. Pedersen – spin/CP combination
- J.P Kinghorn-Taenzer – VH(WW*)
- P.H. Sales De Bruin - A ->Zh->lltautau
- O. Nackenhorst - ttH (bb)

Backup

LHC and ATLAS

Outstanding LHC performance

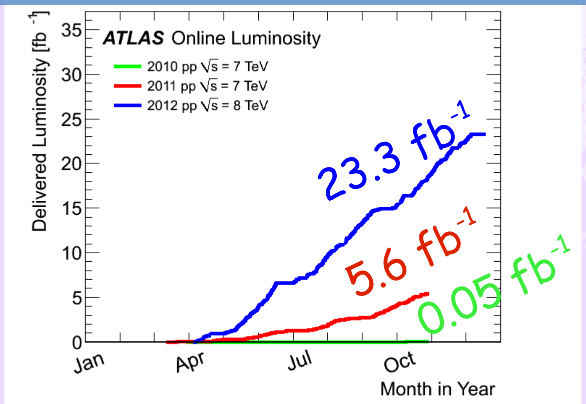

Peak L_{inst}: $7.7\text{x}10^{33}$ $\text{cm}^{-2}\ \text{s}^{-1}$

Excellent ATLAS performance

Data-taking efficiency: 93%

Good quality data fraction used for analysis: 95.8%

Challenge: harsh pile-up conditions [trigger, computing, reconstruction of physics objects]

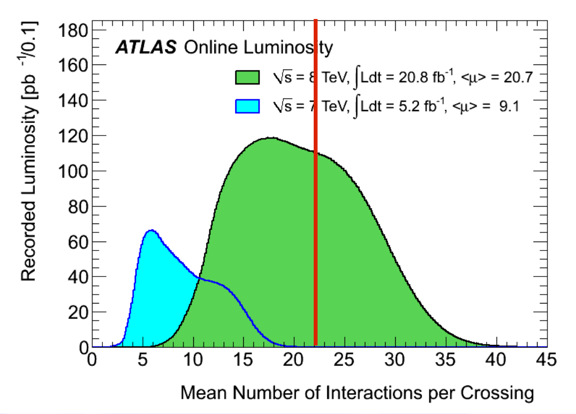

Z→μμ event with 25 reconstructed vertices

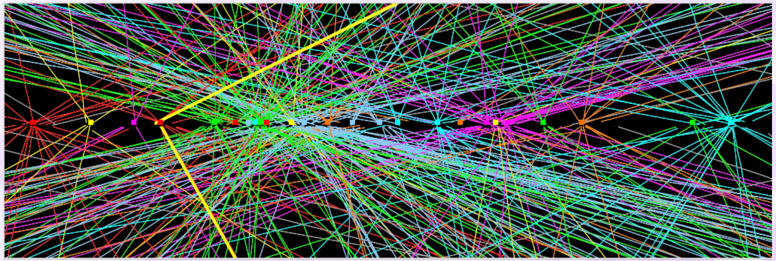

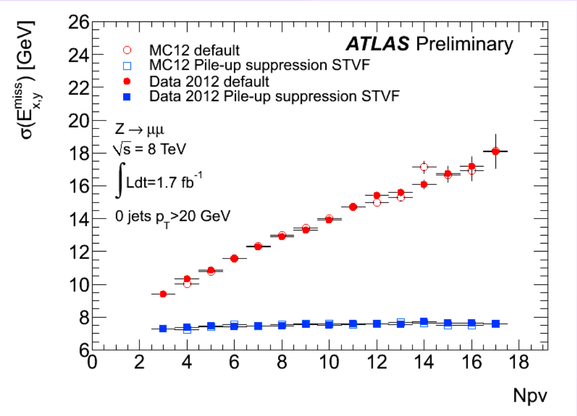

Hγγ categories

signal strength

mass measurement

Category	n_{sig}	FWHM [GeV]	σ_{eff} [GeV]	b in $\pm\sigma_{eff90}$	s/b [%]	$s/\sqrt{b}$
$\sqrt{s}$=8 TeV						
Inclusive	402.	3.69	1.67	10670	3.39	3.50
Unconv. central low p_{Tt}	59.3	3.13	1.35	801	6.66	1.88
Unconv. central high p_{Tt}	7.1	2.81	1.21	26.0	24.6	1.26
Unconv. rest low p_{Tt}	96.2	3.49	1.53	2624	3.30	1.69
Unconv. rest high p_{Tt}	10.4	3.11	1.36	93.9	9.95	0.96
Unconv. transition	26.0	4.24	1.86	910	2.57	0.78
Conv. central low p_{Tt}	37.2	3.47	1.52	589	5.69	1.38
Conv. central high p_{Tt}	4.5	3.07	1.35	20.9	19.4	0.88
Conv. rest low p_{Tt}	107.2	4.23	1.88	3834	2.52	1.56
Conv. rest high p_{Tt}	11.9	3.71	1.64	144.2	7.44	0.89
Conv. transition	42.1	5.31	2.41	1977	1.92	0.85

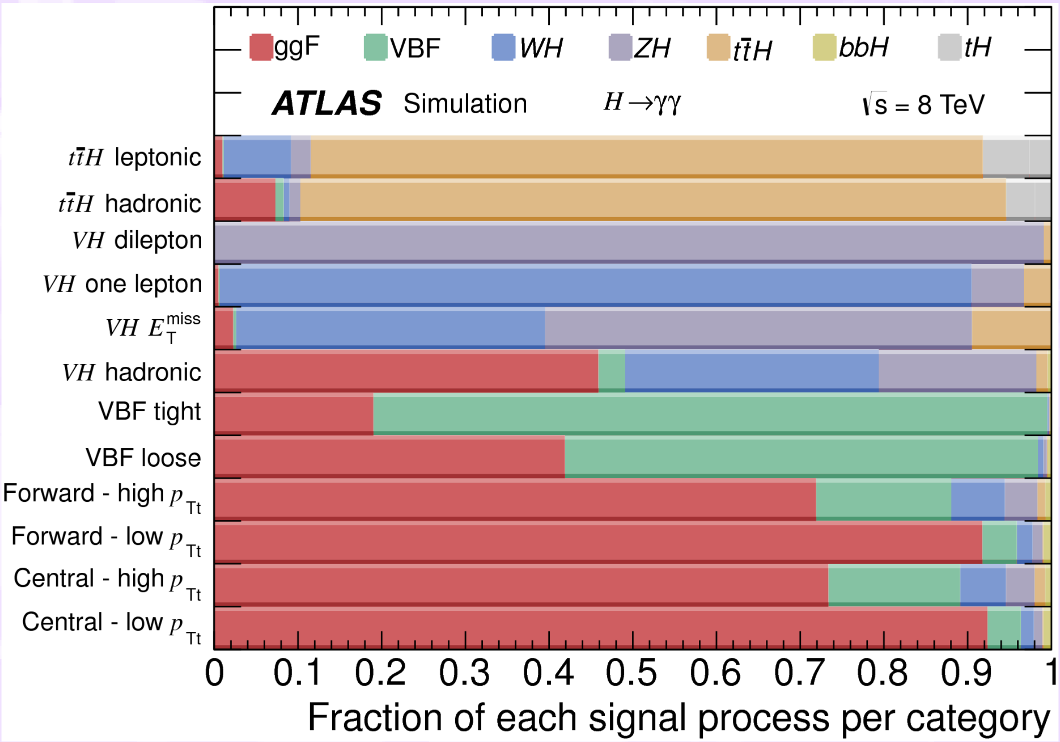

no production mode categories for the x-section measurement

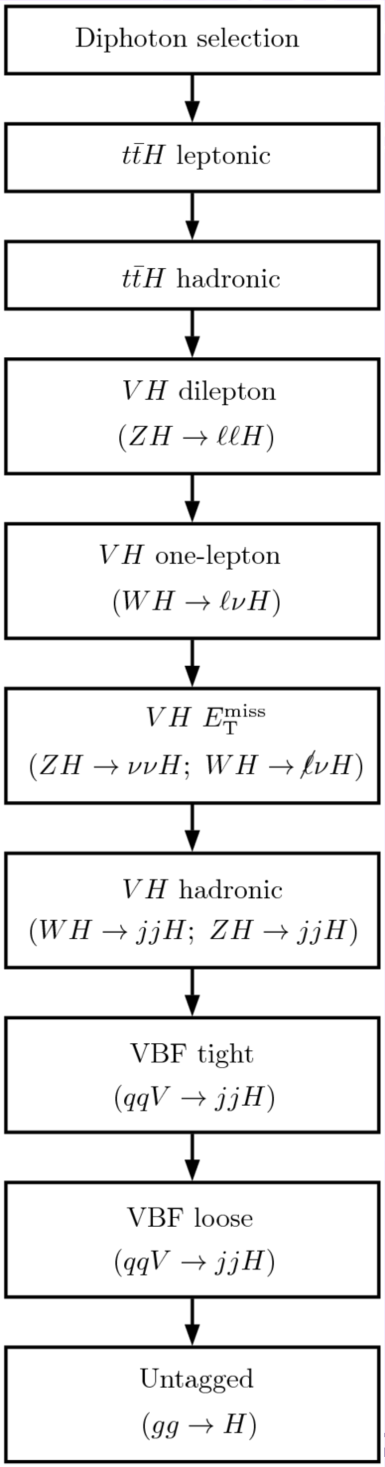

Δφjj

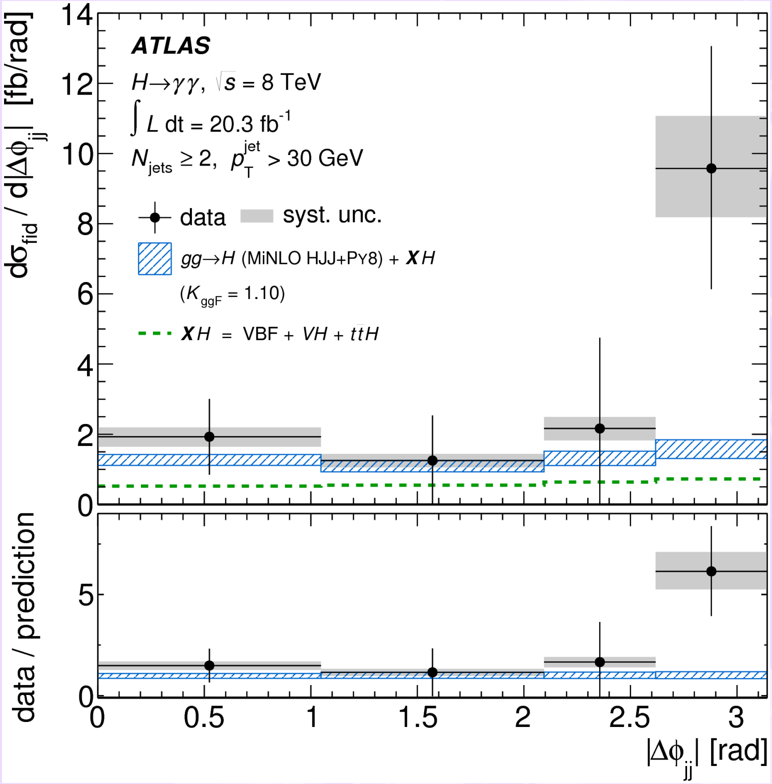

- To further quantify the structure of the azimuthal angle between the two jets, an asymmetry is defined as

$$A_{\Delta\phi} = \frac{\sigma(|\Delta\phi| < \frac{\pi}{3}) - \sigma(\frac{\pi}{3} < |\Delta\phi| < \frac{2\pi}{3}) + \sigma(|\Delta\phi| > \frac{2\pi}{3})}{\sigma(|\Delta\phi| < \frac{\pi}{3}) + \sigma(\frac{\pi}{3} < |\Delta\phi| < \frac{2\pi}{3}) + \sigma(|\Delta\phi| > \frac{2\pi}{3})}$$

- The measured asymmetry in data is
  AΔφ = 0.72 +0.23 −0.29 (stat.) +0.01−0.02 (syst.)

- This can be compared to the Standard Model prediction of
  ASM Δφ = 0.43 ± 0.02
  which is constructed from the Minlo HJJ prediction for gluon fusion and the standard VBF, V H and ttH ¯ predictions

HZZ categories

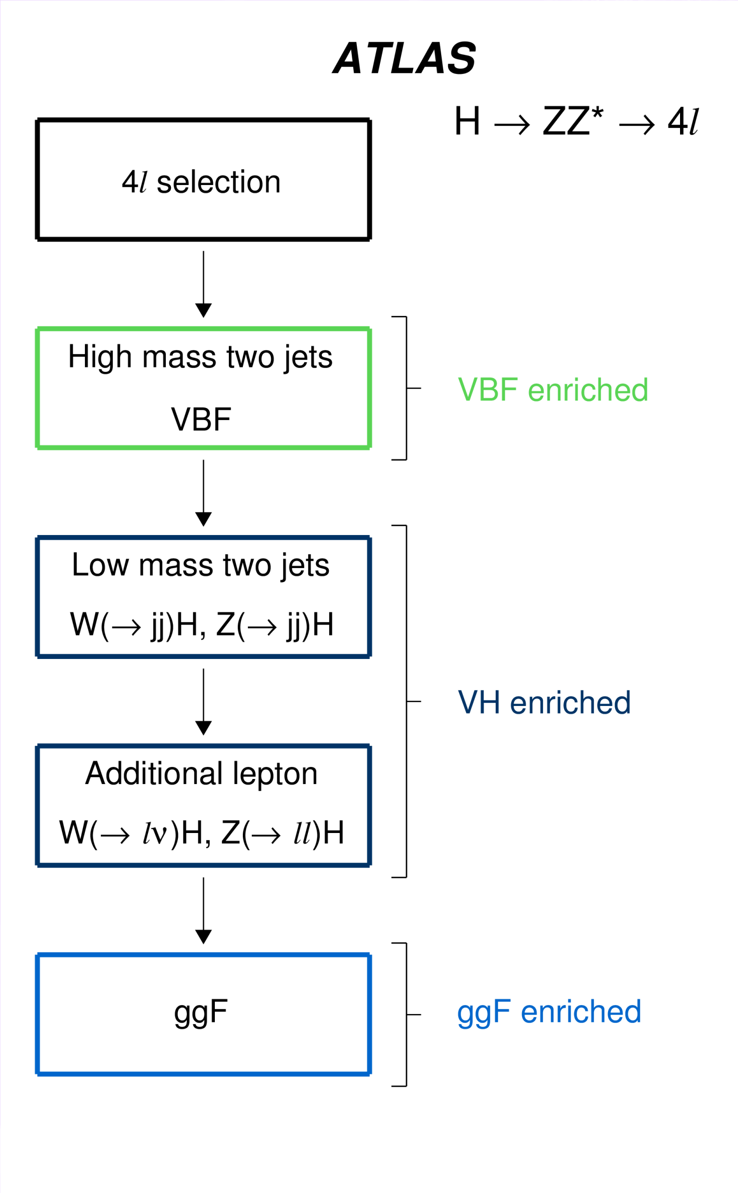

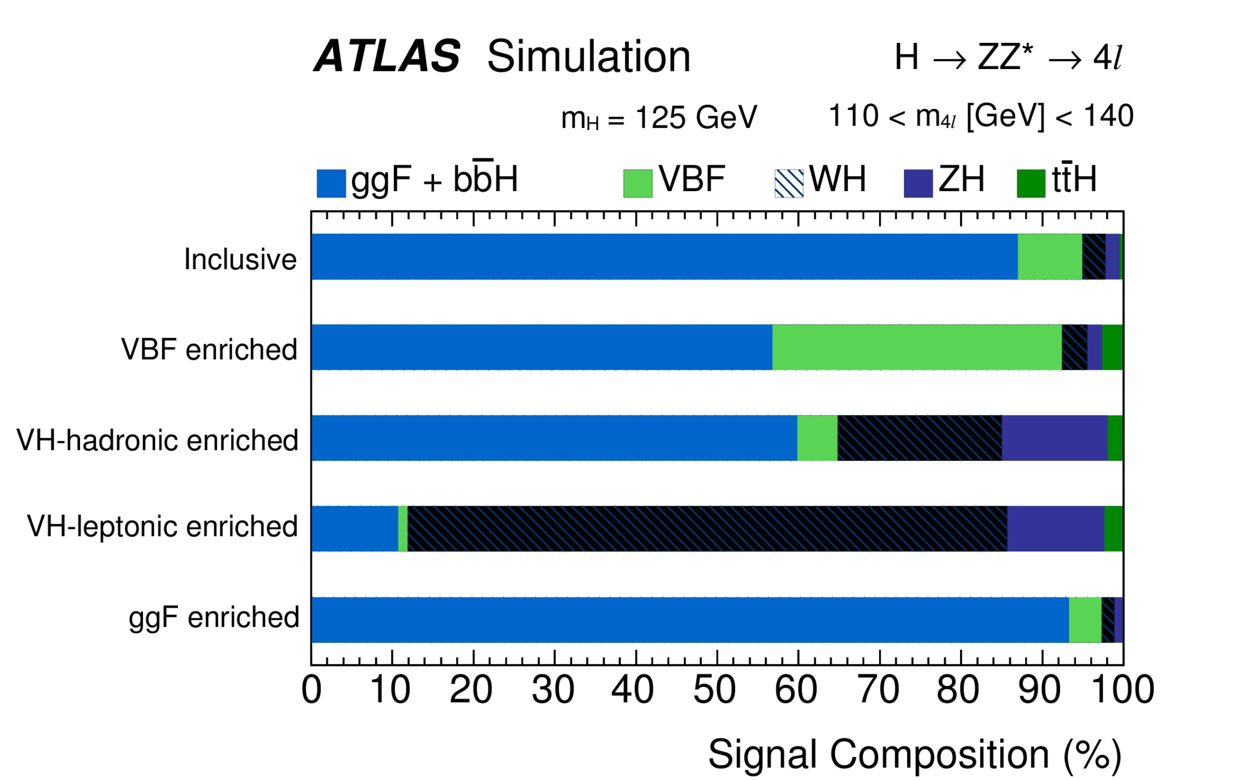

HZZ selection/categorization effect

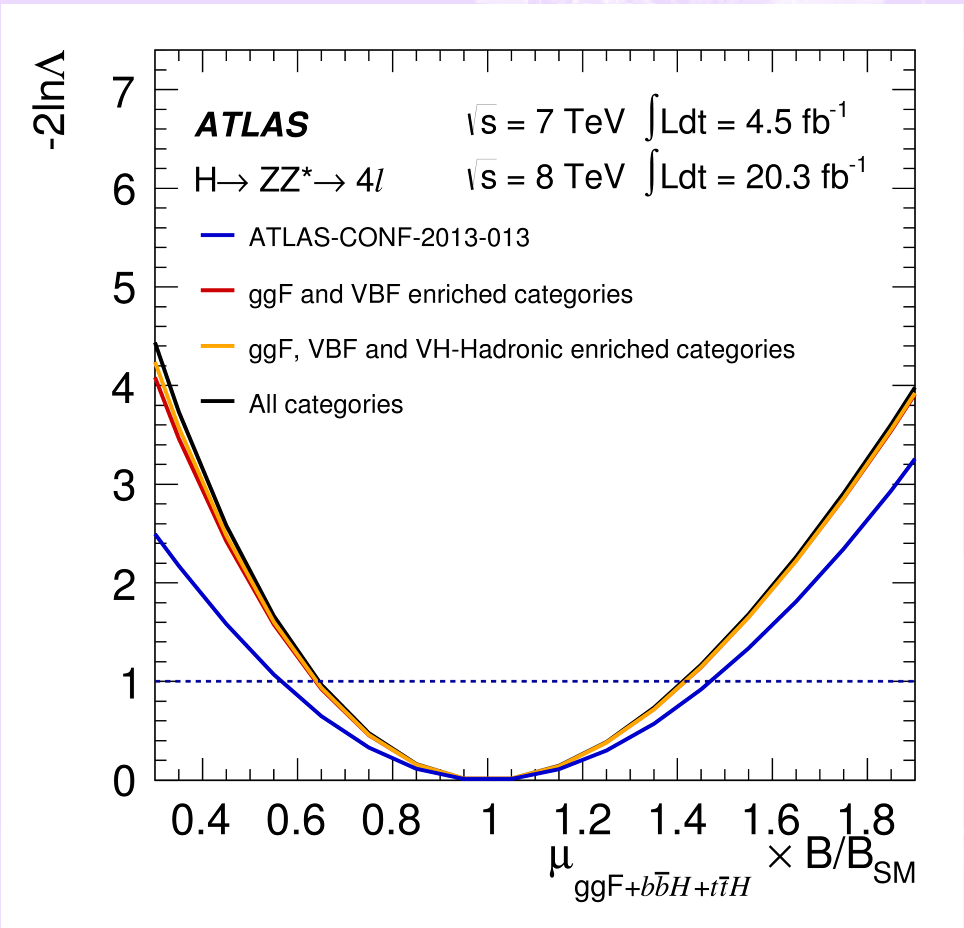

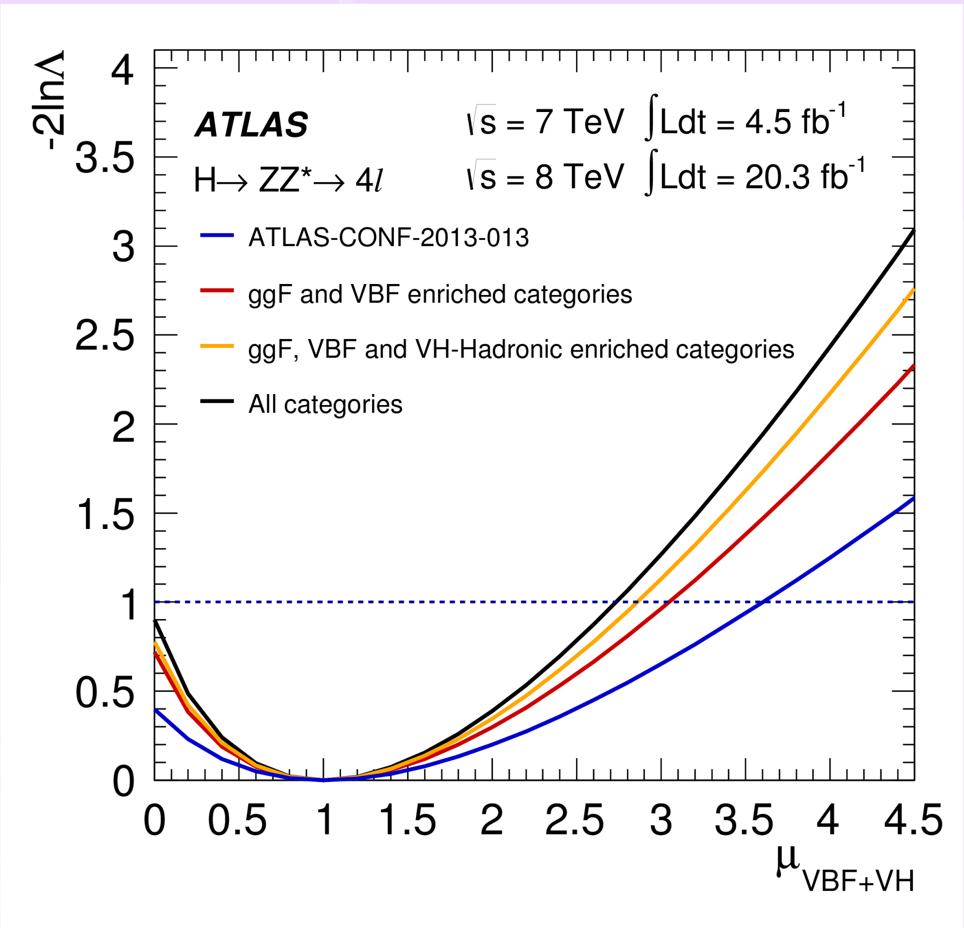

WW regions

(a) Signal region categories

SR category i				Fit var.
n_j, flavor	$\otimes\, m_{\ell\ell}$	$\otimes\, p_{\mathrm{T}}^{\ell 2}$	$\otimes\, \ell_2$	
$n_j = 0$				
$e\mu$	$\otimes\, [10, 30, 55]$	$\otimes\, [10, 15, 20, \infty]$	$\otimes\, [e, \mu]$	m_{T}
$ee/\mu\mu$	$\otimes\, [12, 55]$	$\otimes\, [10, \infty]$		m_{T}
$n_j = 1$				
$e\mu$	$\otimes\, [10, 30, 55]$	$\otimes\, [10, 15, 20, \infty]$	$\otimes\, [e, \mu]$	m_{T}
$ee/\mu\mu$	$\otimes\, [12, 55]$	$\otimes\, [10, \infty]$		m_{T}
$n_j \geq 2$ ggF				
$e\mu$	$\otimes\, [10, 55]$	$\otimes\, [10, \infty]$		m_{T}
$n_j \geq 2$ VBF				
$e\mu$	$\otimes\, [10, 50]$	$\otimes\, [10, \infty]$		O_{BDT}
$ee/\mu\mu$	$\otimes\, [12, 50]$	$\otimes\, [10, \infty]$		O_{BDT}

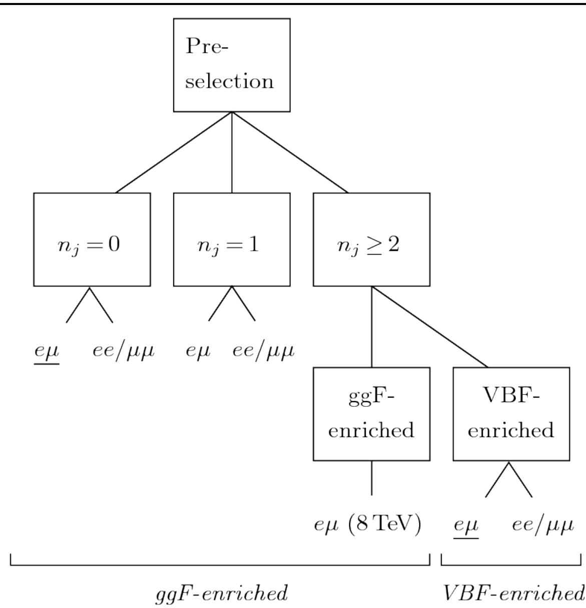

(b) Control regions that are profiled (•) and nonprofiled (○)

CR	Profiled?	Sample	Notable differences vs. SR
$n_j = 0$			
WW	•	$e\mu$	$55 < m_{\ell\ell} < 110$, $\Delta\phi_{\ell\ell} < 2.6$, $p_{\mathrm{T}}^{\ell 2} > 15$
Top	○	$e\mu$	$n_j = 0$ after presel., $\Delta\phi_{\ell\ell} < 2.8$
Wj	○	Same	One anti-identified ℓ
jj	○	Same	Two anti-identified ℓ
VV	•	$e\mu$	Same-charge ℓ (only used in $e\mu$)
DY, $ee/\mu\mu$	•	$ee/\mu\mu$	$f_{\mathrm{recoil}} > 0.1$ (only used in $ee/\mu\mu$)
DY, $\tau\tau$	•	$e\mu$	$m_{\ell\ell} < 80$, $\Delta\phi_{\ell\ell} > 2.8$
$n_j = 1$			
WW	•	$e\mu$	$m_{\ell\ell} > 80$, $\lvert m_{\tau\tau} - m_Z \rvert > 25$, $p_{\mathrm{T}}^{\ell 2} > 15$
Top	•	$e\mu$	$n_b = 1$
Wj	○	Same	One anti-identified ℓ
jj	○	Same	Two anti-identified ℓ
VV	•	$e\mu$	Same-charge ℓ (only used in $e\mu$)
DY, $ee/\mu\mu$	•	$ee/\mu\mu$	$f_{\mathrm{recoil}} > 0.1$ (only used in $ee/\mu\mu$)
DY, $\tau\tau$	•	$e\mu$	$m_{\ell\ell} < 80$, $m_{\tau\tau} > m_Z - 25$
$n_j \geq 2$ ggF			
Top	•	$e\mu$	$m_{\ell\ell} > 80$
Wj	○	Same	One anti-identified ℓ
jj	○	Same	Two anti-identified ℓ
DY, $\tau\tau$	•	$e\mu$	$m_{\ell\ell} < 70$, $\Delta\phi_{\ell\ell} > 2.8$
$n_j \geq 2$ VBF			
Top	•	Both	$n_b = 1$
Wj	○	Same	One anti-identified ℓ
jj	○	Same	Two anti-identified ℓ
DY, $ee/\mu\mu$	○	$ee/\mu\mu$	$E_{\mathrm{T}}^{\mathrm{miss}} < 45$ (only used in $ee/\mu\mu$)
DY, $\tau\tau$	○	Both	$m_{\ell\ell} < 80$, $\lvert m_{\tau\tau} - m_Z \rvert < 25$

WW

Objective		ggF-enriched			VBF-enriched
		$n_j = 0$	$n_j = 1$	$n_j \geq 2$ ggF	$n_j \geq 2$ VBF
Preselection	All n_j	$p_{\mathrm{T}}^{\ell 1} > 22$ for the leading lepton ℓ_1			
		$p_{\mathrm{T}}^{\ell 2} > 10$ for the subleading lepton ℓ_2			
		Opposite-charge leptons			
		$m_{\ell\ell} > 10$ for the $e\mu$ sample			
		$m_{\ell\ell} > 12$ for the $ee/\mu\mu$ sample			
		$\lvert m_{\ell\ell} - m_Z \rvert > 15$ for the $ee/\mu\mu$ sample			
		$p_{\mathrm{T}}^{\mathrm{miss}} > 20$ for $e\mu$	$p_{\mathrm{T}}^{\mathrm{miss}} > 20$ for $e\mu$	$p_{\mathrm{T}}^{\mathrm{miss}} > 20$ for $e\mu$	No MET requirement for $e\mu$
		$E_{\mathrm{T,rel}}^{\mathrm{miss}} > 40$ for $ee/\mu\mu$	$E_{\mathrm{T,rel}}^{\mathrm{miss}} > 40$ for $ee/\mu\mu$	-	-
Reject backgrounds	DY	$p_{\mathrm{T,rel}}^{\mathrm{miss\,(trk)}} > 40$ for $ee/\mu\mu$	$p_{\mathrm{T,rel}}^{\mathrm{miss\,(trk)}} > 35$ for $ee/\mu\mu$	-	$p_{\mathrm{T}}^{\mathrm{miss}} > 40$ for $ee/\mu\mu$
		$f_{\mathrm{recoil}} < 0.1$ for $ee/\mu\mu$	$f_{\mathrm{recoil}} < 0.1$ for $ee/\mu\mu$	-	$E_{\mathrm{T}}^{\mathrm{miss}} > 45$ for $ee/\mu\mu$
		$p_{\mathrm{T}}^{\ell\ell} > 30$	$m_{\tau\tau} < m_Z - 25$	$m_{\tau\tau} < m_Z - 25$	$m_{\tau\tau} < m_Z - 25$
		$\Delta\phi_{\ell\ell,\mathrm{MET}} > \pi/2$	-	-	-
	Misid.	-	$m_{\mathrm{T}}^{\ell} > 50$ for $e\mu$	-	-
	Top	$n_j = 0$	$n_b = 0$	$n_b = 0$	$n_b = 0$
		-	-	-	$p_{\mathrm{T}}^{\mathrm{sum}}$ inputs to BDT
		-	-	-	$\Sigma\, m_{\ell j}$ inputs to BDT
VBF topology		-	-	See Sec. IV D for rejection of VBF & VH ($W, Z \to jj$), where $H \to WW^*$	m_{jj} inputs to BDT Δy_{jj} inputs to BDT $\Sigma\, C_\ell$ inputs to BDT $C_{\ell 1} < 1$ and $C_{\ell 2} < 1$ $C_{j3} > 1$ for j_3 with $p_{\mathrm{T}}^{j3} > 20$ $O_{\mathrm{BDT}} \geq -0.48$
$H \to WW^* \to \ell\nu\ell\nu$ decay topology		$m_{\ell\ell} < 55$	$m_{\ell\ell} < 55$	$m_{\ell\ell} < 55$	$m_{\ell\ell}$ inputs to BDT
		$\Delta\phi_{\ell\ell} < 1.8$	$\Delta\phi_{\ell\ell} < 1.8$	$\Delta\phi_{\ell\ell} < 1.8$	$\Delta\phi_{\ell\ell}$ inputs to BDT
		No m_{T} requirement	No m_{T} requirement	No m_{T} requirement	m_{T} inputs to BDT

arXiv:1506.06641

VH(WW)

Category	Signal significance Z_0: Exp. Z_0	Obs. Z_0	Obs. Z_0	Observed signal strength μ: μ	Tot. err. +	Tot. err. −	Syst. err. +	Syst. err. −	μ
4ℓ	0.41	1.9		**4.9**	4.6	3.1	1.1	0.40	
2SFOS	0.19	0		**−5.9**	6.8	4.1	0.33	0.72	
1SFOS	0.36	2.5		**9.6**	8.1	5.4	2.1	0.64	
3ℓ	0.79	0.66		**0.72**	1.3	1.1	0.40	0.29	
1SFOS and 3SF	0.41	0		**−2.9**	2.7	2.1	1.2	0.92	
0SFOS	0.68	1.2		**1.7**	1.9	1.4	0.51	0.29	
2ℓ	0.59	2.1		**3.7**	1.9	1.5	1.1	1.1	
DFOS	0.54	1.2		**2.2**	2.0	1.9	1.0	1.1	
SS2jet	0.17	1.4		**7.6**	6.0	5.4	3.2	3.2	
SS1jet	0.27	2.3		**8.4**	4.3	3.8	2.3	2.0	

VH production
2.5σ significance
(0.9σ expected)

$$\mu = 3.0\ ^{+1.3}_{-1.1}\ (\text{stat})\ ^{+1.0}_{-0.7}\ (\text{syst})$$

Category	Signal significance Z_0: Exp. Z_0	Obs. Z_0	Obs. Z_0	Observed signal strength μ: μ	Tot. err. +	Tot. err. −	Syst. err. +	Syst. err. −	μ
ggF	4.4	4.2		**0.98**	0.29	0.26	0.22	0.18	
VBF	2.6	3.2		**1.28**	0.55	0.47	0.32	0.25	
VH	0.93	2.5		**3.0**	1.6	1.3	0.95	0.65	
WH only	0.77	1.4		**2.1**	1.9	1.6	1.2	0.79	
ZH only	0.30	2.0		**5.1**	4.3	3.1	1.9	0.89	
ggF+VBF+VH	5.9	6.5		**1.16**	0.24	0.21	0.18	0.15	

mass uncertainties

Systematic	Uncertainty on m_H [MeV]
LAr syst on material before presampler (barrel)	70
LAr syst on material after presampler (barrel)	20
LAr cell non-linearity (layer 2)	60
LAr cell non-linearity (layer 1)	30
LAr layer calibration (barrel)	50
Lateral shower shape (conv)	50
Lateral shower shape (unconv)	40
Presampler energy scale (barrel)	20
ID material model ($\|\eta\| < 1.1$)	50
$H \rightarrow \gamma\gamma$ background model (unconv rest low p_{Tt})	40
$Z \rightarrow ee$ calibration	50
Primary vertex effect on mass scale	20
Muon momentum scale	10
Remaining systematic uncertainties	70
Total	180

EFT

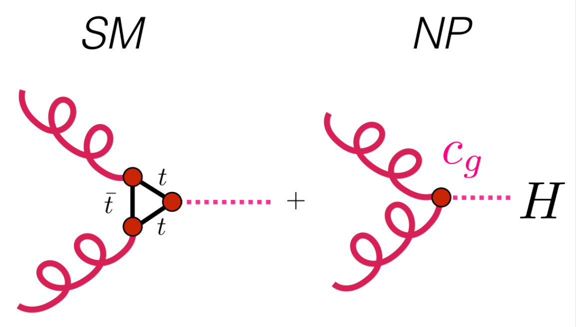

SM
NP
t
$\bar{t}$
t
c_g
H

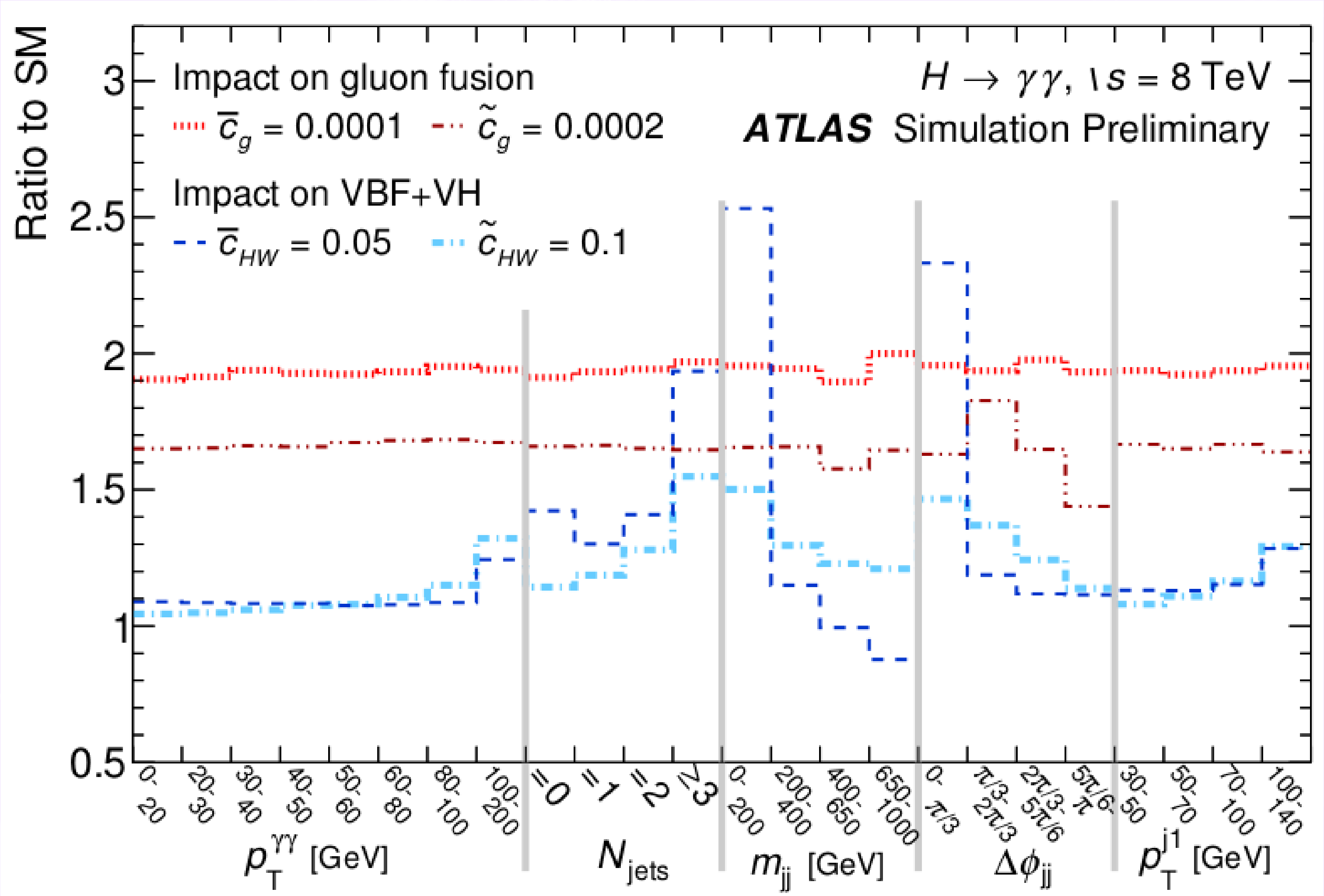

Ratio to SM
Impact on gluon fusion
$\bar{c}_g$ = 0.0001
$\tilde{c}_g$ = 0.0002
Impact on VBF+VH
$\bar{c}_{HW}$ = 0.05
$\tilde{c}_{HW}$ = 0.1
$H \rightarrow \gamma\gamma$, $\sqrt{s}$ = 8 TeV
ATLAS Simulation Preliminary
$p_T^{\gamma\gamma}$ [GeV]
N_{jets}
m_{jj} [GeV]
$\Delta\phi_{jj}$
p_T^{j1} [GeV]

arXiv:1506.05669

Higgs spin/parity

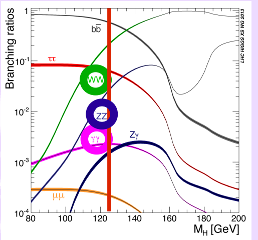

- SM $J^P = 0^+$ tested against alternative models [non-SM spin-0 and spin-2 with different choices of QCD couplings] using spin/CP sensitive variables
- Data favor the SM $J^P = 0^+$ hypotheses in the individual channels and exclude all alternative hypotheses with their combination [R.Polifka's talk]

combine

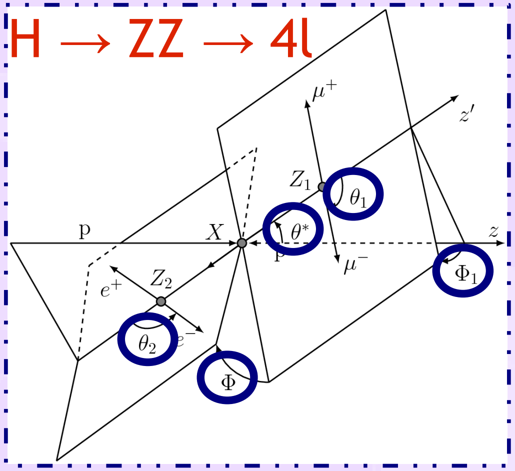

Eur. Phys. J. C75 231 (2015)

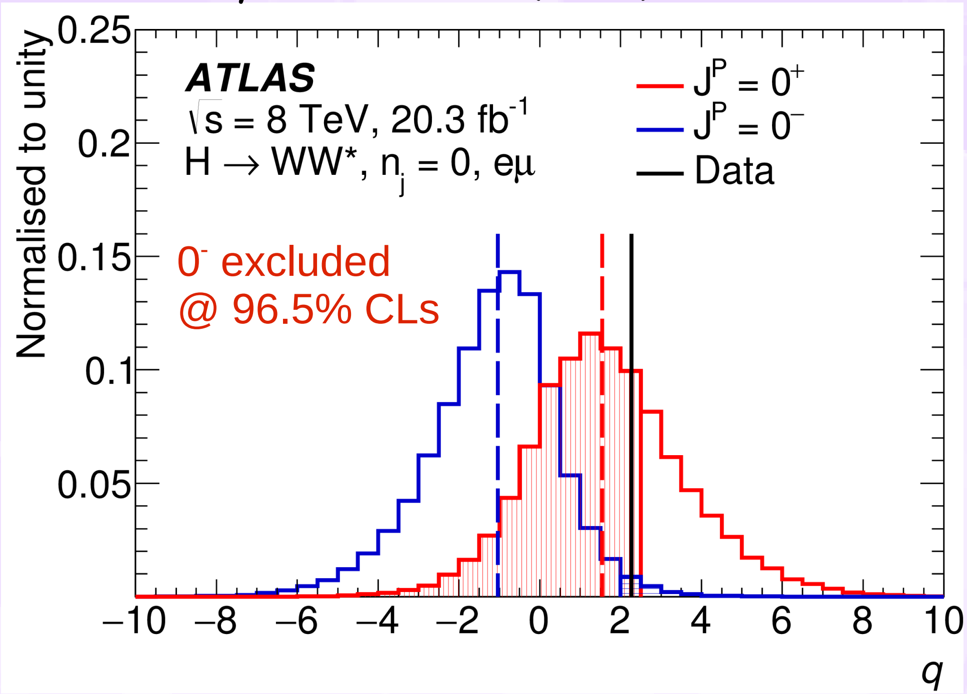

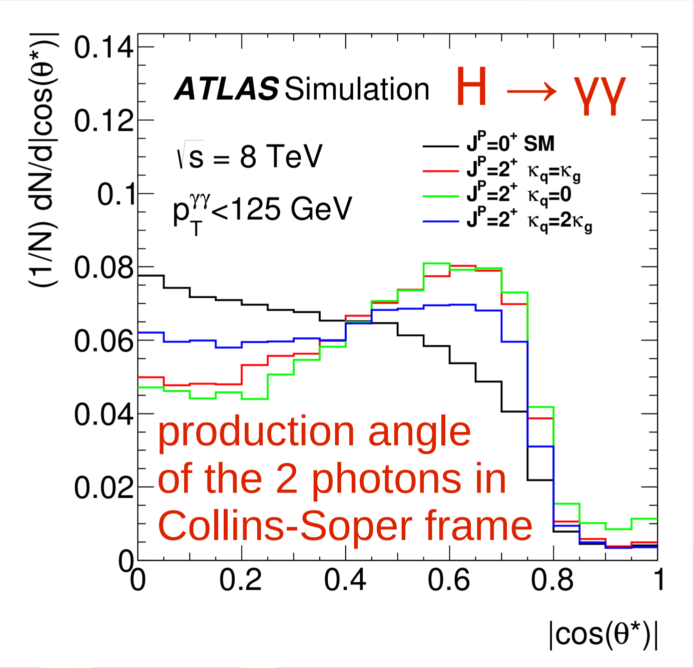

arXiv:1506.05669

CP mixing

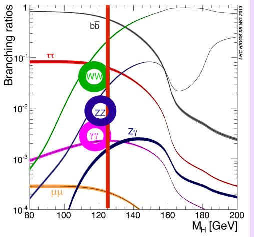

- Probe possible presence of BSM terms in the HVV tensor structure of the spin-0 resonance

$$\mathcal{L}_0^V = \{c_\alpha \kappa_{SM}[\frac{1}{2} g_{HZZ} Z_\mu Z^\mu + g_{HWW} W^+_\mu W^{-}\mu] - \frac{1}{4}\frac{1}{\Lambda}[c_\alpha \kappa_{HZZ} Z_{\mu\nu}Z^{\mu\nu} + s_\alpha \kappa_{AZZ} Z_{\mu\nu}\tilde{Z}^{\mu\nu}] - \frac{1}{2}\frac{1}{\Lambda}[c_\alpha\kappa_{HWW}W^+_{\mu\nu}W^{-\mu\nu} + s_\alpha \kappa_{AWW} W^+_{\mu\nu}\tilde{Z}^{-\mu\nu}]\}$$

SM coupling

BSM CP-odd coupling

BSM CP-even coupling

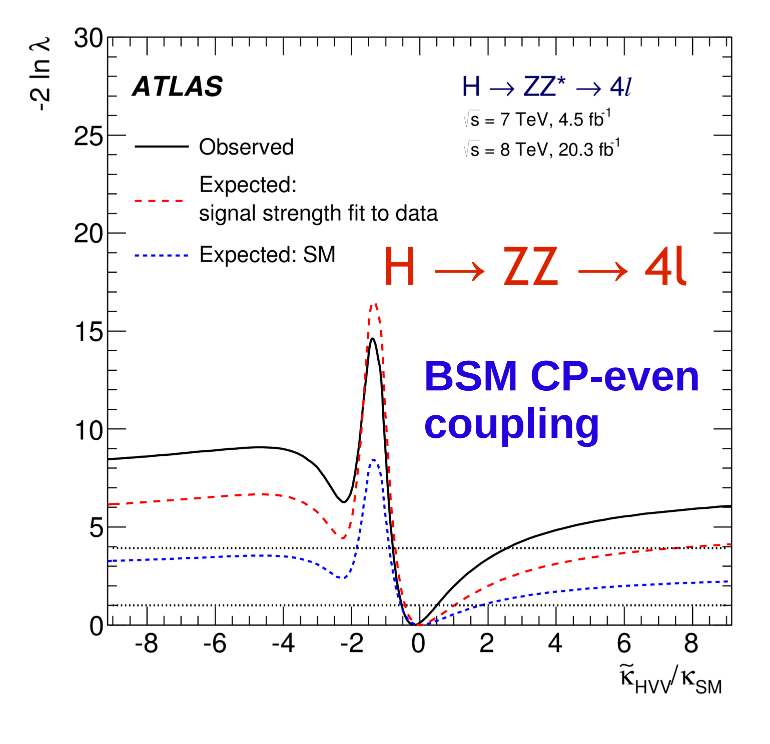

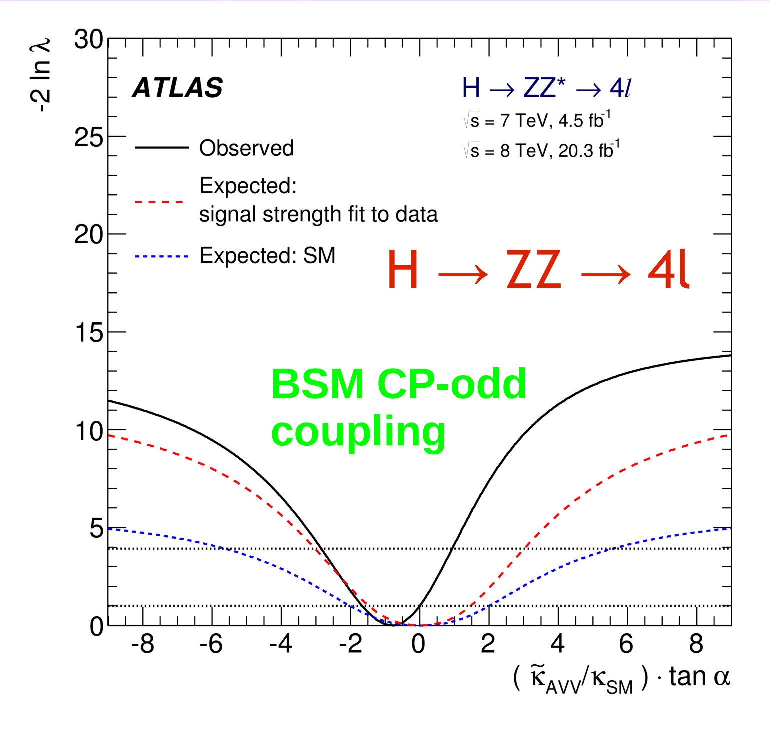

spin/CP individual results

Tested Hypothesis	$p^{\rm alt}_{{\rm exp},\mu=1}$	$p^{\rm alt}_{{\rm exp},\mu=\hat{\mu}}$	$p^{\rm SM}_{\rm obs}$	$p^{\rm alt}_{\rm obs}$	Obs. $\mathrm{CL_s}$ (%)
			$H \rightarrow \gamma\gamma$		
$2^+(\kappa_q = \kappa_g)$	0.13	$7.5 \cdot 10^{-2}$	0.13	0.34	39
$2^+(\kappa_q = 0;\ p_{\rm T} < 300 GeV)$	$4.3 \cdot 10^{-4}$	$< 3.1 \cdot 10^{-5}$	0.16	$2.9 \cdot 10^{-4}$	$3.5 \cdot 10^{-2}$
$2^+(\kappa_q = 0;\ p_{\rm T} < 125 GeV)$	$9.4 \cdot 10^{-2}$	$5.6 \cdot 10^{-2}$	0.23	0.20	26
$2^+(\kappa_q = 2\kappa_g;\ p_{\rm T} < 300 GeV)$	$9.1 \cdot 10^{-4}$	$< 3.1 \cdot 10^{-5}$	0.16	$8.6 \cdot 10^{-4}$	0.10
$2^+(\kappa_q = 2\kappa_g;\ p_{\rm T} < 125 GeV)$	0.27	0.24	0.20	0.54	68
			$H \rightarrow WW^* \rightarrow e\nu\mu\nu$		
Tested Hypothesis	$p^{\rm alt}_{{\rm exp},\mu=1}$	$p^{\rm alt}_{{\rm exp},\mu=\hat{\mu}}$	$p^{\rm SM}_{\rm obs}$	$p^{\rm alt}_{\rm obs}$	Obs. $\mathrm{CL_s}$ (%)
0^+_h	0.31	0.29	0.91	$2.7 \cdot 10^{-2}$	29
0^-	$6.4 \cdot 10^{-2}$	$3.2 \cdot 10^{-2}$	0.65	$1.2 \cdot 10^{-2}$	3.5
$2^+(\kappa_q = \kappa_g)$	$6.4 \cdot 10^{-2}$	$3.3 \cdot 10^{-2}$	0.25	0.12	16
$2^+(\kappa_q = 0;\ p_{\rm T} < 300 GeV)$	$1.5 \cdot 10^{-2}$	$4.0 \cdot 10^{-3}$	0.55	$3.0 \cdot 10^{-3}$	0.6
$2^+(\kappa_q = 0;\ p_{\rm T} < 125 GeV)$	$5.6 \cdot 10^{-2}$	$2.9 \cdot 10^{-2}$	0.42	$4.4 \cdot 10^{-2}$	7.5
$2^+(\kappa_q = 2\kappa_g;\ p_{\rm T} < 300 GeV)$	$1.5 \cdot 10^{-2}$	$4.0 \cdot 10^{-3}$	0.52	$3.0 \cdot 10^{-3}$	0.7
$2^+(\kappa_q = 2\kappa_g;\ p_{\rm T} < 125 GeV)$	$4.4 \cdot 10^{-2}$	$2.2 \cdot 10^{-2}$	0.69	$7.0 \cdot 10^{-3}$	2.2
			$H \rightarrow ZZ^* \rightarrow 4\ell$		
Tested Hypothesis	$p^{\rm alt}_{{\rm exp},\mu=1}$	$p^{\rm alt}_{{\rm exp},\mu=\hat{\mu}}$	$p^{\rm SM}_{\rm obs}$	$p^{\rm alt}_{\rm obs}$	Obs. $\mathrm{CL_s}$ (%)
0^+_h	$3.2 \cdot 10^{-2}$	$5.2 \cdot 10^{-3}$	0.80	$3.6 \cdot 10^{-4}$	0.18
0^-	$8.0 \cdot 10^{-3}$	$3.6 \cdot 10^{-4}$	0.88	$1.2 \cdot 10^{-5}$	$1.0 \cdot 10^{-2}$
$2^+(\kappa_q = \kappa_g)$	$3.3 \cdot 10^{-2}$	$5.7 \cdot 10^{-4}$	0.91	$3.6 \cdot 10^{-5}$	$4.0 \cdot 10^{-2}$
$2^+(\kappa_q = 0;\ p_{\rm T} < 300 GeV)$	$3.9 \cdot 10^{-2}$	$9.0 \cdot 10^{-3}$	0.95	$2.7 \cdot 10^{-5}$	$5.4 \cdot 10^{-2}$
$2^+(\kappa_q = 0;\ p_{\rm T} < 125 GeV)$	$4.6 \cdot 10^{-2}$	$1.1 \cdot 10^{-2}$	0.93	$3.0 \cdot 10^{-5}$	$4.3 \cdot 10^{-2}$
$2^+(\kappa_q = 2\kappa_g;\ p_{\rm T} < 300 GeV)$	$4.6 \cdot 10^{-2}$	$1.1 \cdot 10^{-2}$	0.66	$3.3 \cdot 10^{-3}$	0.97
$2^+(\kappa_q = 2\kappa_g;\ p_{\rm T} < 125 GeV)$	$5.0 \cdot 10^{-2}$	$1.3 \cdot 10^{-2}$	0.88	$3.2 \cdot 10^{-4}$	0.27